Correspondence

Cross-Layer Network Lifetime Maximization in Interference-Limited WSNs

Halil Yetgin, *Student Member, IEEE*,
Kent Tsz Kan Cheung, *Student Member, IEEE*,
Mohammed El-Hajjar, *Member, IEEE*, and
Lajos Hanzo, *Fellow, IEEE*

***Abstract*—In wireless sensor networks (WSNs), the network lifetime (NL) is a crucial metric since the sensor nodes usually rely on limited energy supply. In this paper, we consider the joint optimal design of the physical, medium access control (MAC), and network layers to maximize the NL of the energy-constrained WSN. The problem of NL maximization can be formulated as a nonlinear optimization problem encompassing the routing flow, link scheduling, transmission rate, and power allocation operations for all active time slots (TSs). The resultant nonconvex rate constraint is relaxed by employing an approximation of the signal-to-interference-plus-noise ratio (SINR), which transforms the problem to a convex one. Hence, the resultant dual problem may be solved to obtain the optimal solution to the relaxed problem with a zero duality gap. Therefore, the problem is formulated in its Lagrangian form, and the Karush–Kuhn–Tucker (KKT) optimality conditions are employed for deriving analytical expressions of the globally optimal transmission rate and power allocation variables for the network topology considered. The nonlinear Gauss–Seidel algorithm is adopted for iteratively updating the rate and power allocation variables using these expressions until convergence is attained. Furthermore, the gradient method is applied for updating the dual variables in each iteration. Using this approach, the maximum NL, the energy dissipation per node, the average transmission power per link, and the lifetime of all nodes in the network are evaluated for a given source rate and fixed link schedule under different channel conditions.**

***Index Terms*—Author, please supply index terms/keywords for your paper. To download the IEEE Taxonomy go to http://www.ieee.org/documents/taxonomy_v101.pdf.**

AQ1

NOMENCLATURE

- Number of nodes: $V = 10$.
- Total number of TSs per link: $N = 18$.
- Path-loss exponent: $m = 4$.
- Euclidean distance between consecutive nodes: $d[\mathrm{m}] = 1$.
- Maximum affordable transmit power per node: $(P_\upsilon)_{\max}[\mathrm{W}] = 50$.
- Spatially periodic link scheduling parameter: $T = \{3, 4, 5, 6, 7, 8, 9\}$.
- Initial battery energy per node: $E_\upsilon[\mathrm{J}] = 5000$.
- Spectral noise power density: $N0[\mathrm{dBm/Hz}] = 1$.
- Power amplifier inefficiency: $\alpha = 0.01$ [26].
- Set of all directed links: $\mathcal{L}$.
- A directed link spanning from transmitter i to receiver j: $l_{i,j}$.
- Set of all sensor nodes: $\mathcal{V}$.
- Network topology incidence matrix: $\mathbf{A}$.
- Emerging link of node υ: $l \in \mathcal{O}(\upsilon)$.
- Incoming link of node υ: $l \in \mathcal{I}(\upsilon)$.
- Network-channel-gain matrix: $\mathbf{G}$.
- Fading gain of the link between transmitter i and receiver j: $H_{i,j} = |h_{i,j}|^2$.
- NL: T_{net}.
- Reciprocal of NL: z.
- Transmission rate of link l in TS n: $r_{l,n}$.
- Transmit power of link l in TS n: $P_{l,n}$.
- Logarithm of the transmit power of link l in TS n: $Q_{l,n} = \log(P_{l,n})$.
- A set of dual variables for energy conservation constraint in (5): $\mathbf{\Omega}$.
- A set of dual variables for transmission rate constraint in (4): $\mathbf{\Psi}$.
- A set of dual variables for transmit power constraint in (6): $\boldsymbol{\vartheta}$.
- A set of dual variables for flow constraint in (3): $\boldsymbol{\mu}$.
- Convergence tolerance of the iterative algorithm: $\epsilon = 10^{-5}$.

I. INTRODUCTION

A wireless sensor network (WSN) is composed of a large number of nodes that monitor physical and environmental conditions and pass their accumulated data through the network to a sink node. There are numerous attractive applications for WSNs, including, for example, designing intelligent highways, controlling air pollution, providing remote health assistance for disabled or elderly people, monitoring river level variations, etc. Each of these applications may be composed of many sensor nodes, each of which consumes considerable amount of energy with sensing, communication, and data processing activities. Since each sensor node drains its limited energy supply as time elapses, the network lifetime (NL) is a crucial metric for these applications and has a major impact on the achievable performance of WSNs. Hence, we aim for analyzing and optimizing the NL of the WSNs under different channel conditions.

The NL defines the total amount of time during which the network is capable of maintaining its full functionality and/or achieves particular objectives during its operation, as exemplified in [1] and [2]. Specifically, the authors of [3]–[5] defined the expiration of the NL as the time instant at which a certain number of nodes in the network depleted their batteries. As a further example, the NL was defined in [6] as the lifetime of the specific sensor node associated with the highest energy consumption rate, whereas the authors of [7]–[9] considered the lifetime of the network to be expired at the particular instant, when the first node's battery was depleted. The NL in [8] was also defined as the instant when the first data collection failure occurred. In this paper, the NL is deemed to be expired, when at least one of the nodes fails due to its discharged battery. Therefore, extending the lifetime of a single node becomes an important and challenging task due to the battery-dependent characteristics of the wireless sensor nodes. This common NL definition is used in this paper since we consider

Manuscript received November 29, 2013; revised August 1, 2014; accepted September 20, 2014. This work was supported in part by the Republic of Turkey Ministry of National Education, by the Industrial Company Members of the Mobile VCE, by the U.K. Engineering and Physical Sciences Research Council, and by the Research Councils U.K. through the India–U.K. Advanced Technology Center of the European Union under the auspices of the Concerto Project and of the European Research Council's Senior Research Fellow Grant. The review of this paper was coordinated by Prof. S. Chen.

The authors are with the School of Electronics and Computer Science, University of Southampton, Southampton SO17 1BJ, U.K. (e-mail: hy3g09@ecs.soton.ac.uk; ktkc106@ecs.soton.ac.uk; meh@ecs.soton.ac.uk; lh@ecs.soton.ac.uk).

Color versions of one or more of the figures in this paper are available online at http://ieeexplore.ieee.org.

Digital Object Identifier 10.1109/TVT.2014.2360361

a network of linearly connected sensor nodes, where a single node's failure may destroy the entire string topology of nodes and, hence, the information of the source cannot be relayed to the sink. When considering the energy dissipated at a sensor node, the battery life is predominantly related to the node's communication activity, where the transmission rate and power must be optimized, while taking into account the battery capacity, the efficiency of the power amplifiers, the receiver and transmitter circuit energy consumption, and other physical layer parameters, including the modulation and coding schemes, the attainable coding gain, the path loss, and so on.

It is widely recognized that transmission at a high transmission rate requires the use of high transmit power, which potentially leads to strong interference among the transmission links [10]. Therefore, the battery depletion of an individual sensor node may become inevitable; hence, the NL may be reduced. However, in large networks, spatial reuse may be adopted for improving the attainable transmission rates at the cost of imposing interference on the network [11]. In this case, link scheduling [12] and multiple-access schemes [13] play a significant role in coordinating the resultant interference. More explicitly, we will demonstrate that scheduling weakly interfering links simultaneously allows the network to maintain a given sum rate at a reduced per-node transmit power, which hence extends the battery life of the nodes and the NL [10]. This is one of the methods routinely employed for taking advantage of spatial reuse to control the level of interference imposed on the network [11]. This method extends the NL since mitigating the interference imposed implies that each transmission requires less power. Therefore, intelligent scheduling should carefully balance the number of simultaneous active links and their transmission duration to keep the required transmit power at a minimum. Furthermore, multihop relaying [14] is capable of conserving the energy of the source node (SN) since intermediate nodes may be employed for reducing the transmission power necessary for maintaining a given end-to-end rate. Hence, we consider the joint optimal design of the transmission rate, transmission power, and scheduling to maximize the NL of energy-constrained WSNs.

There is a paucity of contributions in the literature on the issue of cross-layer NL optimization in the context of WSNs. Hoesel *et al.* [15] proposed a cross-layer approach for jointly optimizing the medium access control (MAC) and routing layer to maximize the NL. Chen and Zhao [8] proposed an efficient MAC protocol that relies both on the channel state information and on the MAC's knowledge of the residual energy to maximize the NL. In [16], Kwon *et al.* investigated the NL maximization problem of WSNs, which jointly considers the physical layer, the MAC layer, and the routing layer in conjunction with the transmission success probability constraint. Additionally, the tradeoff between NL maximization and application performance was studied in [17] by using cross-layer optimization. A similar study also investigated the tradeoff between the energy consumption and application-layer performance with the aid of cross-layer optimization of WSNs [18]. Another cross-layer approach conceived for maximizing the NL was proposed in [19], where MAC-aware routing optimization schemes were designed for WSNs that are capable of multichannel access. In [20], Li *et al.* invoked random linear network coding for the lifetime maximization of wireless networks within a fixed-rate system for communicating over both additive white Gaussian noise (AWGN) and Rayleigh fading channels. A different approach to NL maximization was introduced in [21], where both contention and sleep control probabilities of the sensor nodes were utilized for formulating the NL maximization problem, while guaranteeing both the required throughput and the signal-to-interference-plus-noise ratio (SINR) requirements. Najimi *et al.* [4] proposed a node selection algorithm for balancing the energy usage of the sensors in a fixed-mode cognitive sensor network. A similar idea

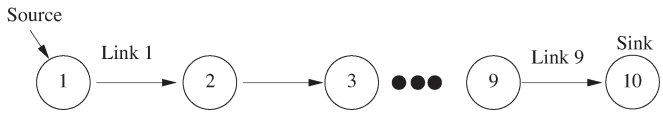

Fig. 1. String topology with $V = 10$ nodes, including an SN and a DN.

to that of the optimal control approach invoked for maximizing the NL with the aid of a carefully selected routing probability was exploited in [9], where all the sensors were configured to deplete their energy exactly at the same time for lifetime maximization. Another similar study advocating an effective transmission scheme was proposed in [22], where both the maximum possible energy efficiency and the best possible energy balancing were maintained with the aid of ant colony optimization.

However, all related work aforementioned considers either non-adaptive, i.e., fixed-mode system, or nonfading channel characteristics. An adaptive system conceived for NL maximization was studied by Wang *et al.* [23], who considered only an interference-free scenario for an AWGN channel by employing the Karush–Kuhn–Tucker (KKT) optimality conditions [24] to the optimal time-division multiple-access (TDMA) NL maximization problem of [12] to derive the analytical expressions of the optimal NL. Madan *et al.* [12] considered an interference-limited scenario relying on an adaptive system, operating in an AWGN channel, but the impact of the fading channel characteristics on the NL was not presented. Wang *et al.* [23] obtained a closed-form solution for a specific network topology. By contrast, a generalized string network topology consisting of an arbitrary number of nodes is considered in our treatise, where we employ the KKT optimality conditions for obtaining the optimal solution to the NL maximization problem using closed-form expressions. Therefore, we are able to derive analytical expressions of the globally optimal NL for a string network operating in an interference-limited scenario, while communicating either over an AWGN or over fading channels for a given link schedule. Furthermore, the maximum NL, the energy dissipation per node, the average transmission power per link, and the lifetime of all nodes in the network may be obtained. We quantify how the maximum NL decreases as a function of the fading statistics due to the poor channel conditions. Furthermore, it is demonstrated that given a certain network sum rate, the simultaneous scheduling of weakly interfering links benefits from the associated spatial reuse by allowing each node to transmit at a lower rate, which requires a reduced transmission power and hence results in a higher NL. Against this backdrop, the novel contributions of this paper can be summarized as follows.

1) The KKT optimality conditions [24] are invoked for deriving the analytical expressions of the globally optimal NL for an interference-limited string topology.
2) In addition to the line-of-sight (LOS) AWGN channel model, the non-LOS Rayleigh block-fading channel model is adopted for studying the effects of fading on the NL.
3) The maximum NL is evaluated, and the energy dissipation per node, the average transmission power per link, and the lifetime of all nodes in the network are quantified for a given link schedule and source rate in both LOS AWGN and non-LOS Rayleigh block-fading channels.
4) The substantial effect of the distance among the consecutive nodes on the NL is also analyzed for lower source rates, when operating in a Rayleigh fading channel. The impact of the interferers is also investigated in the context of higher source rates.

The remainder of this paper is organized as follows. Section II describes our system model and the constraints of the optimization problem considered. Our problem formulation and solution approach

Links \ Slots	1	2	3	4	5	6	7	8	9	10	11	12	13	14	15	16	17	18
l_{1-2}	●+			●			●			●+			●			●		
l_{2-3}		●+			●			●			●+			●			●	
l_{3-4}			●+			●			●			●+			●			●
l_{4-5}	●			●+			●			●			●+			●		
l_{5-6}		●			●+			●			●			●+			●	
l_{6-7}			●			●+			●			●			●+			●
l_{7-8}	●			●			●+			●			●			●+		
l_{8-9}		●			●			●+			●			●			●+	
l_{9-10}			●			●			●+			●			●			●+

●: T=3 spatially periodic link schedule +: T=9 spatially periodic link schedule

Fig. 2. Spatially periodic link schedule with time sharing parameter $T = 3$ and $T = 9$ when $N = 18$ and $V = 10$.

are presented in Section III, and our numerical results are shown in Section IV. Our conclusions are provided in Section V.

II. System Model

Here, we first describe the network model,[1] which relies on a string topology.[2] Second, we detail our transceiver model in Section II-B, where we evaluate the NL for transmission over both AWGN and block-fading channels. Moreover, our transmission scheduling strategy is also described and exemplified at the end of Section II-B.

A. Network Model

We consider a string topology composed of V sensor nodes, where the SN and the destination node (DN) are linearly connected by intermediate nodes. An example of this string topology for $V = 10$ is shown in Fig. 1; hence, the number of links is $L = V - 1 = 9$.

Each link is unidirectional, and the antenna of each node is omnidirectional. The network can be modeled as a directed graph $\mathcal{G} = \{\mathcal{V}, \mathcal{L}\}$, where $\mathcal{V} = \{1, 2, 3, \ldots, V\}$ is the set of all sensor nodes, and $\mathcal{L} = \{l_{1,2}, l_{2,3}, \ldots, l_{V-1,V}\}$ is the set of all directed links in the network. Here, $l_{i,j}$ represents the directed link spanning from the transmitter node i to receiver node j. Therefore, the topology can be modeled with the aid of an incidence matrix of the graph $\mathcal{G}$ given by $\mathbf{A} \in \mathbf{R}^{|\mathcal{V}|\times|\mathcal{L}|}$. The entries $a_{v,l}$ of $\mathbf{A}$ are given by

$$a_{v,l} = \begin{cases} 1, & \text{if } v \text{ is the transmitter of link } l \\ -1, & \text{if } v \text{ is the receiver of link } l \\ 0, & \text{otherwise.} \end{cases} \quad (1)$$

We consider a single commodity flow. Therefore, by the conservation of flow, the constraint $\sum_{l\in\mathcal{O}(v)}(\sum_{n=1}^{N} r_{l,n}) = \sum_{l\in\mathcal{I}(v)} \times (\sum_{n=1}^{N} r_{l,n})$ may be written for each node v in the absence of an external source or sink, where N is the total number of time slots (TSs) per TDMA frame, and $r_{l,n}$ is the transmission rate of link l in TS n. Additionally, $l \in \mathcal{O}(v)$ denotes the emerging link, and $l \in \mathcal{I}(v)$ represents the incoming link of node v.

[1]Our network model is a centralized one, where the sink node is assumed to be a control center.

[2]A string topology is chosen since, in this simple scenario, the effect of transmission variables on the NL can be explicitly exposed and analyzed. Our string topology scenario is also capable of providing insights concerning a randomly distributed network with many nodes since a specific set of nodes can be assumed to constitute a single route of the randomly distributed network.

B. Channel Model and MAC Layer Scheme

In each TS n, each node can only act as a transmitter or a receiver. Each transmitter is only allowed to communicate with a single receiver, which cannot receive from other nodes in the same TS. This is due to the half-duplex nature of the transceivers, where nodes communicate on the same shared wireless channel. The channel gain of the link between transmitter i and receiver j is given by $G_{i,j} = 1/(d_{i,j})^m$, where $d_{i,j}$ is the distance between nodes i and j, whereas the path-loss exponent is $m = 4$. These channel gains are arranged into a network-channel-gain matrix denoted by $\mathbf{G}$. Each node v is capable of transmitting at a power less than the maximum power of that node denoted by $(P_v)_{\max}$. The total energy dissipation at a node cannot exceed the initial battery energy of that node. No node is allowed to simultaneously transmit multiple data packets, and the link quality is defined by the SINR.

The LOS AWGN channel is modeled by a certain propagation path-loss law and a fixed noise power at the receivers. Given a specific link l, the SINR is denoted by Γ_l in the AWGN channel model. The maximum achievable rate per unit bandwidth is $r_l = \log(1 + K \cdot \Gamma_l)$ given in nats/s/Hz, where $K = -1.5/\log(5\text{BER})$ [25], and BER represents the target bit error ratio (BER) required by the system. Therefore, the SINR is given by [13] $\Gamma_{l_{i,j},n} = G_{i,j}P_{i,n}/(\sum_{i'\neq i} G_{i',j}P_{i',n} + N_0)$, where $P_{i,n}$ is the transmission power of node i in TS n. Furthermore, K is assumed to incorporate the coding gain and any other gain factors, which is a suitable model for M-ary quadrature amplitude modulation (MQAM) associated with $M \geq 4$ [25]. The factor K is assumed absorbed into the gain matrix $\mathbf{G}$.

On the other hand, when considering fading channels, the channel of each link is modeled as a multiplicative Rayleigh fading channel contaminated by the noise added at the receivers. We consider block fading or quasi-static fading, where the fading gain is kept constant throughout the TDMA frame for the link, which represents slowly fading channels, i.e., low Doppler pedestrian speeds. This requires a modification of the SINR used in AWGN channels, which is formulated as [25] $\widetilde{\Gamma}_{l_{i,j},n} = H_{i,j}G_{i,j}P_{i,n}/(\sum_{i'\neq i} H_{i',j}G_{i',j}P_{i',n} + N_0)$, where $H_{i,j} = |h_{i,j}|^2$ is the fading gain of the link between transmitter i and receiver j.

We assume a link scheduling associated with spatially periodic time sharing [12], where we consider a distance T between links that are transmitting in the same TS, and the link is reactivated after every T TSs. Fig. 2 shows the spatially periodic link scheduling for $T=3$ and $T=9$. For $T=3$, at the first TS, links $l_{1,2}, l_{4,5}, l_{7,8}$ are simultaneously scheduled, and each link is activated six times in total in TSs of 1, 4, 7, 10, 13, and 16. On the other hand, for $T=9$, each TS has only a single active transmission, and each link is activated twice, as shown in Fig. 2.

III. Problem Formulation and Solution

Having discussed the assumptions and constraints in Section II, the NL maximization problem [12] can be formulated as in

$$\min. \quad z \tag{2}$$

$$\text{s.t.} \quad \mathbf{A}(\mathbf{r}_1+\mathbf{r}_2+\cdots+\mathbf{r}_N)=\mathbf{s}\cdot N \tag{3}$$

$$\left(\frac{N_0}{G_{i,j}}\cdot e^{r_{l_{i,j},n}-Q_{l_{i,j},n}} + \sum_{l_{i',j'}\in\mathcal{L}_n, i'\neq i}\frac{G_{i',j}}{G_{i,j}}\cdot e^{r_{l_{i,j},n}+Q_{l_{i',j',n}}-Q_{l_{i,j},n}}\right) - 1 \leq 0 \quad \forall n,\ l\in\mathcal{L}_n \tag{4}$$

$$\sum_{n=1}^{N}\left(\sum_{l\in\mathcal{O}(v)\cap\mathcal{L}_n}\left((1+\alpha)\cdot e^{Q_{l_{i,j},n}}+P_{\text{ct}}\right) + \sum_{l\in\mathcal{I}(v)\cap\mathcal{L}_n}P_{\text{cr}}\right)\leq z\cdot E_v\cdot N \quad \forall v \tag{5}$$

$$Q_{l_{i,j},n}\leq\log((P_i)_{\max}),\ l\in\mathcal{L}_n \tag{6}$$

$$\mathbf{r}_n\geq 0 \quad \forall n \tag{7}$$

$$r_{l_{i,j},n}=0 \quad \forall l\notin\mathcal{L}_n \tag{8}$$

where (4) has been modified, so that it constitutes a strictly convex constraint. See the Nomenclature list on the first page of this paper for the specific parameters utilized in our simulations.

The links that are active in TS n are denoted by the set $\mathcal{L}_n$, and $\mathbf{s}=[s_1,0,\ldots,-s_1]^T$ is the source rate vector, where the first and last elements are nonzero but the remaining elements are set to zero because the first node is the SN and the last node is the DN, and the other nodes act as relay nodes (RN). The variables of the optimization problem are z, $Q_{l,n}$, and $r_{l,n}$, for $l\in\mathcal{L}_n$, $n=1,\ldots,N$. The vector of rate variables associated with TS n is given by $\mathbf{r}_n=[r_{l_{1,2},n}, r_{l_{2,3},n},\ldots,r_{l_{V-1,V},n}]^T$. Assuming that the transmitter and receiver circuits do not dissipate energy, we can set $P_{\text{ct}}=0$ and $P_{\text{cr}}=0$, where P_{ct} and P_{cr} denote the power required by the transmitter and receiver circuits, respectively. Furthermore, we denote the power amplifier inefficiency as α [26]. The lifetime of a node in the network is denoted by T_v, which corresponds to the time during which the node runs out of battery. The NL is defined as the time during which at least one node completely drains its battery, i.e., we have $T_{\text{net}}=\min_{v\neq V, v\in\mathcal{V}}. T_v$. The objective function (OF) and the constraints of the optimization problem are as follows.

1) *Objective function—Minimization of reciprocal of the NL*: In (2), we minimize z so that the NL is maximized. Here, we used a minimization technique in our problem. We can rewrite (5) as $\sum_{n=1}^{N}(\sum_{l\in\mathcal{O}(v)\cap\mathcal{L}_n}((1+\alpha)\cdot e^{Q_{l_{i,j},n}}+P_{\text{ct}})+\sum_{l\in\mathcal{I}(v)\cap\mathcal{L}_n}P_{\text{cr}})\leq(1/T_{\text{net}})\cdot E_v\cdot N$, and we can multiply the left-hand side of the inequality by T_{net}, but the multiplication of the two optimization variables is in general nonconvex. Therefore, we use a change of variable and minimize $z=1/T_{\text{net}}$, which keeps the right-hand side of the inequality linear and left-hand side convex.
2) *Flow conservation constraint*: In (3), using matrix $\mathbf{A}$ with entries given by 1 ensures that flow conservation is preserved, and physically, this means that the information generated at the SN has to arrive at the DN.
3) *Transmission rate constraint*: We have to satisfy the rate constraint of our interference-limited scenario for each link of the same TS in (4).
4) *Energy conservation constraint*: Each sensor node can dissipate at most the initial amount of battery energy, which we set to 5000 J. Therefore, in (5), the energy conservation constraint is given for each node.
5) *Transmit power constraint*: Equation (6) represents the transmission power at a node, which has to be less than the maximum affordable transmit power of that node.
6) *No transmission*: Finally, the transmission rate of nodes that are not scheduled for transmission is set to zero in (8).

The optimization problem is solved for the sake of finding the optimal scheme for transmission over each link for a given link schedule, which is defined by the spatially periodic time sharing discussed in Section II-B. However, to obtain the globally optimal solutions, we wish to show that (2)–(8) represent a convex optimization problem, composed of a convex OF, convex inequality constraint functions, and affine equality constraint functions. It is clear that (3) and (8) are affine, (2) and (5)–(7) are convex, and (4) is strictly convex [24]. Therefore, (2)–(8) define a strictly convex optimization problem that has a unique solution. We can convert the problem into its Lagrangian form and rely on the KKT optimality conditions [24] for deriving the analytical expressions of the globally optimal transmission scheme for the string network topology of Fig. 1.

A. Karush–Kuhn–Tucker Optimality Conditions

Lets us define the sets of the optimization variables and of the Lagrangian multipliers as $\boldsymbol{R}=\{r_{l_{1,2},1},\ldots,r_{l_{V-1,V},N}\}$, $\boldsymbol{Q}=\{Q_{l_{1,2},1},\ldots,Q_{l_{V-1,V},N}\}$, $\boldsymbol{\mu}=\{\mu_1,\ldots,\mu_V\}$, $\boldsymbol{\Psi}=\{\psi_{l_{1,2},1},\ldots,\psi_{l_{V-1,V},N}\}$, $\boldsymbol{\Omega}=\{\omega_1,\ldots,\omega_{V-1}\}$, and $\boldsymbol{\vartheta}=\{\vartheta_{l_{1,2},1},\ldots,\vartheta_{l_{V-1,V},N}\}$. Thus, the partial Lagrangian of (2)–(8) is given by (9), shown at the bottom of the next page, where ω_v, $\psi_{l_{i,j},n}$, and $\vartheta_{l_{i,j},n}$, μ_v are the dual variables associated with the constraints (3)–(6), respectively. Constraints (7) and (8) are taken into account, when deriving the optimal primal variables.

The KKT conditions for (9) are given by (10)–(16), shown at the bottom of the next page, where $\mathcal{I}^{-1}(l)$ denotes the node associated with the incoming link l, and $\mathcal{O}^{-1}(l)$ represents the node associated with the outgoing link l. Since the primal problem is convex, if $z,\boldsymbol{R},\boldsymbol{Q},\boldsymbol{\Omega},\boldsymbol{\Psi},\boldsymbol{\vartheta},\boldsymbol{\mu}$ represent arbitrary points that satisfy the KKT optimality conditions given by the primal feasibility in (3)–(6), the dual feasibility of (16), the complementary slackness in (13)–(15), and the first-order optimality in (10)–(12), then $z,\boldsymbol{R},\boldsymbol{Q}$ are primal optimal, and $\boldsymbol{\Omega},\boldsymbol{\Psi},\boldsymbol{\vartheta},\boldsymbol{\mu}$ are dual optimal[3] with zero duality gap[4] [24].

[3]Optimal solution of the primal (original) problem is expressed as primal optimal and the dual problem provides us a lower bound on the optimal value of the original optimization problem. Hence, the dual optimal is a lower bound on the primal optimal.

[4]The duality gap is defined as the difference between the optimal primal and optimal dual solutions.

B. Problem Solution

From (11) and (12), the optimal values of $\boldsymbol{Q}$ and $\boldsymbol{R}$ in iteration $(t+1)$ are given by (17) and (18), respectively, shown at the bottom of the next page. Note that, due to the interference terms in (11) and (12), each optimal variable in $\boldsymbol{Q}$ and $\boldsymbol{R}$ is dependent on the other variables of $\boldsymbol{Q}$ and $\boldsymbol{R}$, which implies that they are interdependent, hence requiring a centralized solution approach.[5] Therefore, the Gauss–Seidel algorithm [27] is utilized for iteratively updating these variables in a circular fashion.

The dual OF is defined as the minimum value of the Lagrangian (9) over $z, \boldsymbol{R}, \boldsymbol{Q}$ given by $g(\boldsymbol{\Omega}, \boldsymbol{\Psi}, \boldsymbol{\vartheta}, \boldsymbol{\mu}) = \inf_{z,\boldsymbol{R},\boldsymbol{Q}} \mathcal{L}(z, \boldsymbol{R}, \boldsymbol{Q}, \boldsymbol{\Omega}, \boldsymbol{\Psi}, \boldsymbol{\vartheta}, \boldsymbol{\mu})$, which is a linear problem even if the primal problem is nonconvex. The dual function $g(\boldsymbol{\Omega}, \boldsymbol{\Psi}, \boldsymbol{\vartheta}, \boldsymbol{\mu})$ may be maximized to find a lower bound for the optimal value of the primal problem. Then, we can write the dual problem as follows:

$$\max_{\boldsymbol{\Omega},\boldsymbol{\Psi},\boldsymbol{\vartheta},\boldsymbol{\mu}} \quad g(\boldsymbol{\Omega}, \boldsymbol{\Psi}, \boldsymbol{\vartheta}, \boldsymbol{\mu})$$
$$\text{s.t.} \quad \boldsymbol{\Omega} \geq 0,\ \boldsymbol{\Psi} \geq 0,\ \boldsymbol{\vartheta} \geq 0$$

which is a linear optimization problem. When the primal problem is convex, this lower bound is tight; therefore, the duality gap is zero. Since the dual problem is continuously differentiable, the gradient ascent algorithm [27] is utilized to solve the maximization problem by simply evaluating a series of closed-form expressions. The gradient

[5]The calculation of both the transmit power and of the rate of a specific node relies on the prior knowledge gleaned from other nodes, possibly from its interferers. Therefore, a control center is required, which handles the variables of the optimization problem and passes the near-instantaneous values of the variables to each of the individual nodes. Compared with a distributed scheme, this centralized solution will impose delay on the system since operations such as channel estimation are required at the initial stage. The near-instantaneous transmission rate and power values computed by the control center constituted by the sink node should be forwarded to each individual node. Therefore, a nonnegligible delay will be imposed on the reception of the sink node.

$$\begin{aligned}\mathcal{L}(z, \boldsymbol{R}, \boldsymbol{Q}, \boldsymbol{\Omega}, \boldsymbol{\Psi}, \boldsymbol{\vartheta}, \boldsymbol{\mu}) = z &+ \sum_{v=1}^{V-1} \omega_v \cdot \left[\sum_{n=1}^{N} \left(\sum_{l \in \mathcal{O}(v) \cap \mathcal{L}_n} \left((1+\alpha) \cdot e^{Q_{l_{i,j},n}} \right) \right) - z \cdot E_v \cdot N \right] \\ &+ \sum_{n=1}^{N} \sum_{l \in \mathcal{L}_n} \psi_{l_{i,j},n} \cdot \left[\left(\frac{N_0}{G_{i,j}} e^{r_{l_{i,j},n} - Q_{l_{i,j},n}} + \sum_{l_{i',j'} \in \mathcal{L}_n, i' \neq i} \frac{G_{i',j}}{G_{i,j}} e^{r_{l_{i,j},n} + Q_{l_{i',j'},n} - Q_{l_{i,j},n}} \right) - 1 \right] \\ &+ \sum_{n=1}^{N} \sum_{l \in \mathcal{L}_n} \vartheta_{l_{i,j},n} \cdot \left[Q_{l_{i,j},n} - \log\left((P_i)_{\max} \right) \right] + \sum_{v=1}^{V} \mu_v \cdot \left[\sum_{l \in \mathcal{I}(v)} \left(\sum_{n=1}^{N} r_{l_{i,j},n} \right) - \sum_{l \in \mathcal{O}(v)} \left(\sum_{n=1}^{N} r_{l_{i,j},n} \right) \right] \end{aligned} \tag{9}$$

$$\frac{\partial \mathcal{L}}{\partial z} = 1 - \sum_{v=1}^{V} \omega_v (E_v \cdot N) = 0 \tag{10}$$

$$\frac{\partial \mathcal{L}}{\partial r_{l_{i,j},n}} = \mu_{\mathcal{I}^{-1}(l)} - \mu_{\mathcal{O}^{-1}(l)} + \psi_{l_{i,j},n} \left(\frac{N_0}{G_{i,j}} e^{r_{l_{i,j},n} - Q_{l_{i,j},n}} + \sum_{l_{i',j'} \in \mathcal{L}_n, i' \neq i} \frac{G_{i',j}}{G_{i,j}} e^{r_{l_{i,j},n} + Q_{l_{i',j'},n} - Q_{l_{i,j},n}} \right) = 0 \quad \forall l, n \tag{11}$$

$$\begin{aligned}\frac{\partial \mathcal{L}}{\partial Q_{l_{i,j},n}} = &\omega_{\mathcal{O}^{-1}(l)} \left((1+\alpha) e^{Q_{l_{i,j},n}} \right) + \vartheta_{l_{i,j},n} \\ &- \psi_{l_{i,j},n} \left(\frac{N_0}{G_{i,j}} e^{r_{l_{i,j},n} - Q_{l_{i,j},n}} + \sum_{l_{i',j'} \in \mathcal{L}_n, i' \neq i} \frac{G_{i',j}}{G_{i,j}} e^{r_{l_{i,j},n} + Q_{l_{i',j'},n} - Q_{l_{i,j},n}} \right) = 0 \quad \forall l, n \end{aligned} \tag{12}$$

$$0 = \sum_{v=1}^{V-1} \omega_v \cdot \left[\sum_{n=1}^{N} \left(\sum_{l \in \mathcal{O}(v) \cap \mathcal{L}_n} \left((1+\alpha) e^{Q_{l_{i,j},n}} \right) \right) - z \cdot E_v \cdot N \right] \tag{13}$$

$$0 = \psi_{l_{i,j},n} \cdot \left[\left(\frac{N_0}{G_{i,j}} e^{r_{l_{i,j},n} - Q_{l_{i,j},n}} + \sum_{l_{i',j'} \in \mathcal{L}_n, i' \neq i} \frac{G_{i',j}}{G_{i,j}} e^{r_{l_{i,j},n} + Q_{l_{i',j'},n} - Q_{l_{i,j},n}} \right) - 1 \right] \quad \forall l, n \tag{14}$$

$$0 = \vartheta_{l_{i,j},n} \cdot \left[Q_{l_{i,j},n} - \log\left((P_i)_{\max} \right) \right] \quad \forall l, n \tag{15}$$

$$\omega_v \geq 0,\ \psi_{l_{i,j},n} \geq 0,\ \vartheta_{l_{i,j},n} \geq 0 \tag{16}$$

of the Lagrangian function defines the search directions at the current point. Each dual variable is incremented in the direction of the positive gradient in (19)–(22), shown at the bottom of the page, where t is the iteration index, and $[\cdot]^+$ denotes $\max(0,\cdot)$. Provided that $\Delta_{\boldsymbol{\Omega}} > 0$, $\Delta_{\boldsymbol{\Psi}} > 0$, $\Delta_{\boldsymbol{\vartheta}} > 0$, and $\Delta_{\boldsymbol{\mu}} > 0$ are sufficiently small positive step sizes, the dual variables $\boldsymbol{\Omega}^t$, $\boldsymbol{\Psi}^t$, $\boldsymbol{\vartheta}^t$, and $\boldsymbol{\mu}^t$ converge to the dual optimal variables $\boldsymbol{\Omega}^*$, $\boldsymbol{\Psi}^*$, $\boldsymbol{\vartheta}^*$, and $\boldsymbol{\mu}^*$, respectively, as $t \to \infty$. In our case, the optimization problem shown in (2)–(8) is strictly convex; thus, the duality gap is zero, and the solution is unique.

IV. Experimental Results

In our experiments, we use the parameters of $d = 1$ m, $\alpha = 0.01$ [26], $K = 1$, $N_0 = 1$ dBm/Hz, $E_v = 5000$ J[6], $(P_i)_{\max} = 50$ W, $N = 18$, $s_1 = \{0.2, 0.3, 0.4, 0.5, 0.6, 0.7\}$ nats/s/Hz $\approx \{0.29, 0.43, 0.58, 0.72, 0.87, 1.01\}$ bits/s/Hz, $T = \{3, 4, 5, 6, 7, 8, 9\}$, convergence tolerance of iterative algorithm $\epsilon = 10^{-5}$.

Fig. 3 shows the NL versus source rate trends for a fixed link schedule and for various spatially periodic time sharing parameters T, where the channel in each link is a LOS AWGN channel characterized by fixed noise power. As expected, the NL decays as a function of the source rate, as shown in Fig. 3. This is because a higher source rate requires a higher transmission rate and, hence, higher transmission power. Furthermore, in our model, the weakly interfering nodes are scheduled to transmit simultaneously; hence, each link becomes capable of transmitting at a lower rate, while still satisfying all the transmit requirements of the SN. This necessitates lower transmission power. Using the $T = 9$ spatially periodic time schedule of Fig. 2 corresponds to a TDMA scheme since there is only a single transmission in each TS, as shown in Fig. 2. However, since the time frame of Fig. 2 consists of 18 TSs, a specific link is scheduled to transmit twice during the whole time frame. Despite the fact that the $T = 9$ link schedule does not impose any interference, it results in the lowest NL according to Fig. 3. Although interference is present in

[6]For example, this is the energy storage capacity of an AAA alkaline long-life battery.

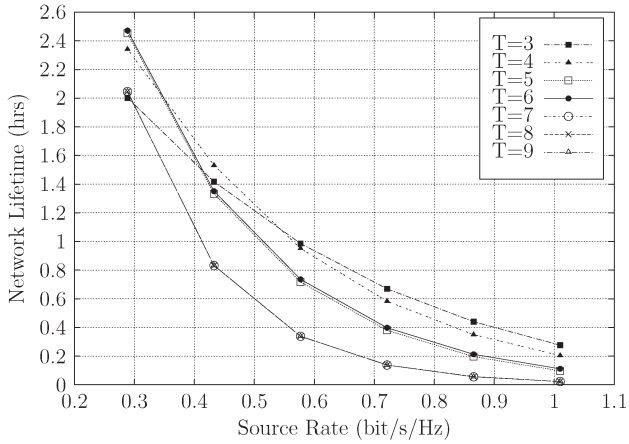

Fig. 3. Network lifetime for different spatially periodic schedules and source rates in the AWGN channel.

$$Q_{l_{i,j},n}^{t+1} = \log\left[\left(\mu_i^t - \mu_j^t - \vartheta_{l_{i,j},n}^t\right)\cdot\left(\omega_i^t(1+\alpha) + \sum_{l_{i',j'}\in\mathcal{L}_n, l_{i',j'}\neq l_{i,j}, i'\geq i} \psi_{l_{i',j'},n}^t\left(\frac{G_{i,j'}}{G_{i',j'}}\cdot e^{r_{l_{i',j'},n}^t - Q_{l_{i',j'},n}^t}\right)\right.\right.$$
$$\left.\left. + \sum_{l_{i',j'}\in\mathcal{L}_n, l_{i',j'}\neq l_{i,j}, i'<i} \psi_{l_{i',j'},n}^t\left(\frac{G_{i,j'}}{G_{i',j'}}\cdot e^{r_{l_{i',j'},n}^t - Q_{l_{i',j'},n}^{t+1}}\right)\right)^{-1}\right] \quad \forall l,n \tag{17}$$

$$r_{l_{i,j},n}^{t+1} = \log\left[\frac{\mu_i^t - \mu_j^t}{\psi_{l_{i,j},n}^t\cdot\left(\frac{N_0}{G_{i,j}} + \sum_{l_{i',j'}\in\mathcal{L}_n, l_{i',j'}\neq l_{i,j}} \frac{G_{i',j}}{G_{i,j}}\cdot e^{Q_{l_{i',j'},n}^{t+1}}\right)}\right] + Q_{l_{i,j},n}^{t+1} \quad \forall l,n \tag{18}$$

$$\omega^{t+1} = \left[\omega^t + \Delta_\omega\left(\sum_{n=1}^{N}\left(\sum_{l\in\mathcal{O}(v)\cap\mathcal{L}_n}\left((1+\alpha)\cdot e^{Q_{l_{i,j},n}}\right)\right) - z\cdot E_v\cdot N\right)\right]^+ \tag{19}$$

$$\psi^{t+1} = \left[\psi^t + \Delta_\psi\left(\left(\frac{N_0}{G_{i,j}}e^{r_{l_{i,j},n} - Q_{l_{i,j},n}} + \sum_{l_{i',j'}\in\mathcal{L}_n, i'\neq i}\frac{G_{i',j}}{G_{i,j}}e^{r_{l_{i,j},n} + Q_{l_{i',j'},n} - Q_{l_{i,j},n}}\right) - 1\right)\right]^+ \tag{20}$$

$$\vartheta^{t+1} = \left[\vartheta^t + \Delta_\vartheta(Q_{l_{i,j},n} - \log((P_i)_{\max}))\right]^+ \tag{21}$$

$$\mu^{t+1} = \left[\mu^t + \Delta_\mu\left(\sum_{l\in\mathcal{I}(v)}\left(\sum_{n=1}^{N} r_{l_{i,j},n}\right) - \sum_{l\in\mathcal{O}(v)}\left(\sum_{n=1}^{N} r_{l_{i,j},n}\right)\right)\right] \tag{22}$$

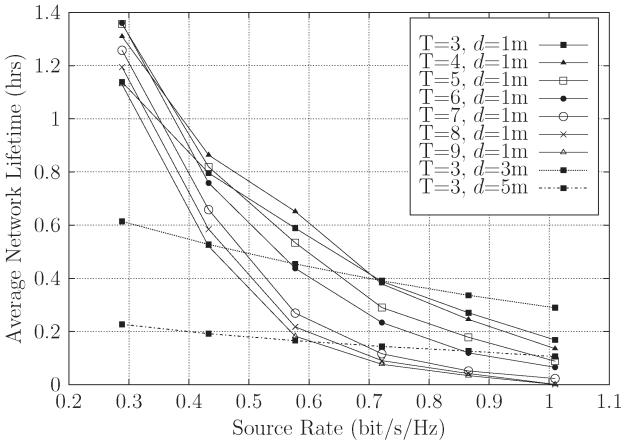

Fig. 4. Network lifetime for different spatially periodic schedules and source rates in a block-fading channel.

the $T = 3$ scenario since each link can be activated three times more often than in the $T = 9$ scenario, each link in the $T = 3$ scenario can be activated at lower transmission power, while still satisfying the end-to-end rate constraint. Therefore, the spatial reuse assisted us in the $T = 3$ scenario for increasing the NL. We can follow Fig. 2 to find out how many transmissions there are per link for a given value of T. For example, the $T = 3$ schedule allows a link to be scheduled six times, which requires a reduced transmission rate, since the total source rate that is delivered over different TSs is using six transmissions. From the flow conservation equality constraint of the optimization problem seen in (3), we have $\mathbf{A}(\mathbf{r}_1 + \mathbf{r}_2 + \cdots + \mathbf{r}_N) = \mathbf{s} \cdot N$. For example, let us assume that the source rate equals to 0.29 bits/s/Hz. Then, we obtain $18 \cdot 0.29 = 5.22$ bits/s/Hz, which has to be divided into six transmissions, corresponding to a 0.87 bits/s/Hz per link transmission rate for $T = 3$. However, when we have $T = 9$, we obtain a 2.61-bits/s/Hz per link transmission rate since a link is only activated twice during the whole time frame. Therefore, the transmission rate per link converges to 0.87 bits/s/Hz for $T = 3$ and 2.61 bits/s/Hz for $T = 9$. Hence, $T = 9$ requires three times as much transmission power as $T = 3$. The required transmit power in weakly interfering links is quite low compared with that for $T = 9$, which is the scenario requiring the highest transmission rate. Hence, again, we surmise that simultaneous scheduling benefits from reduced transmission power due to its reduced transmission rate per link. This is because the spatially periodic schedule allows us to schedule more transmissions during the same TS or to activate the same link more than once in different TSs. This explains the steep decay of the NL for $T = 9$.

When considering the effects of node density on a given fixed link schedule, we expect a network supporting less than $V = 10$ nodes to be exposed to less interference. Therefore, the transmission power of each link can be reduced without reducing the end-to-end transmission rate, which results in a higher NL. On the other hand, upon increasing the node density, we expect the NL to decrease since more interferers are introduced, but the same transmission rate is required.

Fig. 4 represents the NL versus source rate tradeoff for a fixed link schedule and for various spatially periodic time sharing parameter values of T when each link obeys an independent and identically distributed Rayleigh block-fading channel. Naturally, the NL was reduced compared with the results of Fig. 3 recorded for an AWGN channel due to requiring higher transmit power to combat the effects of fading. We also analyzed the impact of the internode distance on the NL for the $T = 3$-based link schedule, when communicating over a Rayleigh fading channel, as shown in Fig. 4. Increasing the distance between the consecutive nodes substantially reduced the NL, particularly for lower source rates. However, quite surprisingly, increasing the distance between the consecutive nodes from 1 to 3 m resulted in an improved NL for higher source rates. This is due to the reduced impact of the interferers located at a higher distance. More explicitly, although the transmit power required had to be increased to satisfy the rate constraint, at the same time the interferers were moved a bit further away. Therefore, the total energy dissipation of the $d = 3$ m scenario is still lower than that of the $d = 1$ m scenario associated with higher source rates.

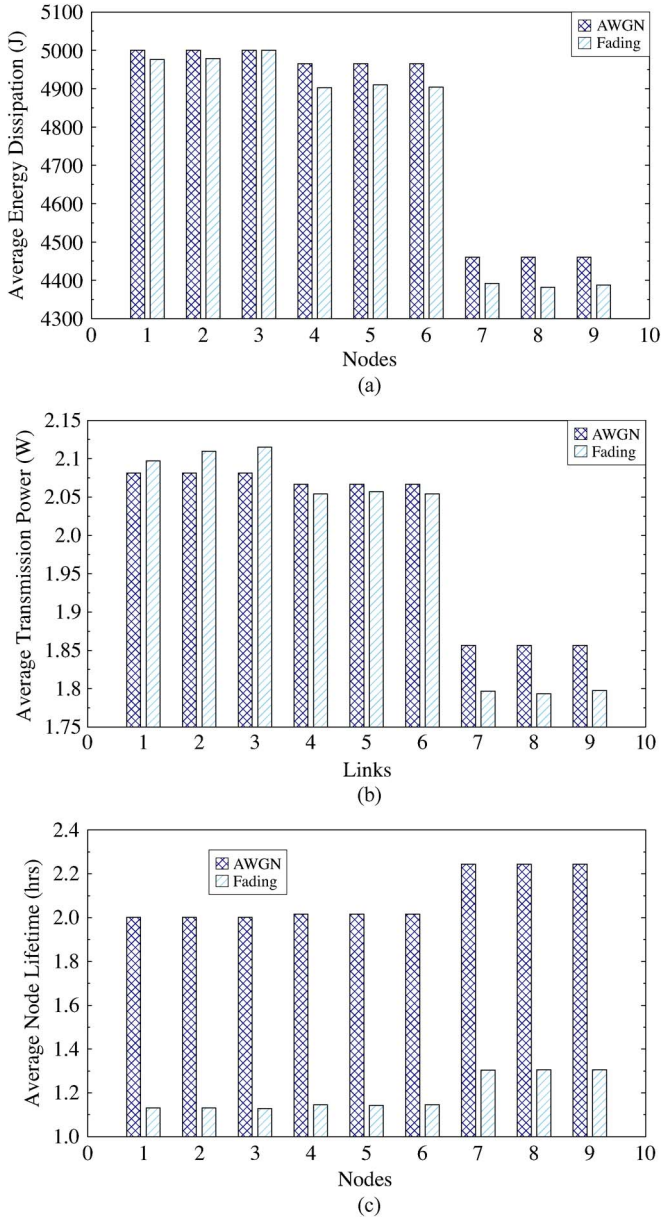

Fig. 5. Energy dissipation per node, average transmit power per link and lifetime of all nodes in the network in both AWGN and fading channels for the $T = 3$ link schedule at a source rate of 0.29 bits/s/Hz. (a) Energy dissipation per node. (b) Average transmit power per link. (c) Lifetime of all nodes in the network.

Furthermore, we comprehensively study the energy dissipation per node, the average transmission power per link, and the lifetime of all sensor nodes in the network. Fig. 5 shows the energy dissipation per node, the average transmission power per link, and the lifetime of all nodes in the network in both AWGN and fading channels for the $T = 3$ link schedule of Fig. 2 at a source rate of 0.29 bits/s/Hz. In the network

topology considered, the transmissions from the first three nodes suffer from the highest amount of interference. This is because their receiving nodes are closer to their potential interferers, when compared with any other sets of nodes. Therefore, to satisfy the flow conservation constraints, these nodes must transmit at higher power, as shown in Fig. 5(b). Thus, in an AWGN channel, the first three nodes in the network dissipate their 5000-J initial amount of energy faster than the other nodes since the energy dissipation is proportional to the transmit power, as shown in Fig. 5(a), whereas in the Rayleigh block-fading channel, the third node runs out of battery first, which also determines the lifetime of the WSNs. The required transmit power of the third link is higher than that in the AWGN channel scenario. This increase in transmit power is required to overcome the effect of fading.

The average transmit power per link is calculated by summing the transmit power values per link and then by dividing it by the number of TSs that the same link was allowed to transmit. For the first three links operating in the AWGN channel, the required transmission power per link is higher than that of the rest of the links. Since requiring a high transmit power results in dissipating more energy, the lifetime of those nodes is reduced, as shown in Fig. 5(c).

Upon comparing the AWGN and fading channel scenarios in Fig. 5, we observe that they follow a similar trend. An observation is that the average transmit power per link of the seventh, eighth, and ninth nodes in Fig. 5(b) is slightly lower for the fading channel than for the AWGN channel. However, interestingly, the average transmit power per link of the third node in Fig. 5(b) recorded for the fading channel is slightly higher than that of the AWGN channel. Therefore, the need for a high transmit power necessitates higher energy dissipation for that particular node. Hence, the NL is reduced, which can also be observed by comparing Figs. 3 and 4. Fig. 3 shows that the NL of the WSN in the AWGN channel recorded for the $T = 3$ link schedule and for 0.29 bits/s/Hz source rate is approximately 2 h. By contrast, Fig. 4 shows that the NL of the WSN operating in a Rayleigh fading scenario for the $T = 3$ link schedule and for 0.29-bits/s/Hz source rate indicates approximately an NL of 1.13 h. This earlier node failure of the fading scenario is due to the poor channel conditions, where the fading required higher transmit power in the third node, as shown in Fig. 5(b). Therefore, this earlier node failure shortened the NL of the WSNs in fading channels.

To put the given results into context, we apply our analysis to the environmental sensor networks of [28], where the relation between glaciers and climate change was studied. In their work, Martinez *et al.* [28] transmit data only once per day for a 0.5-s time slot. In this specific application and considering our results in Fig. 5 for $T = 3$ and a source rate of 0.29 bits/s/Hz, the battery will serve communications for 7200 s, which means that the NL will be around four years and three months in the LOS AWGN channel. We also consider what NL we can achieve if the environmental conditions are more challenging and the channel is exposed to the severe environments mentioned in [28], which may be modeled by a non-LOS Rayleigh block-fading channel. Activating the communication channel once per day in fading conditions will lead us to an NL of around two years and six months.

V. Conclusion

We evaluated the optimal NL in an interference-limited scenario for an optimal transmit rate and power, when considering the so-called spatially periodic time sharing scheme of Fig. 2. The maximization of NL was formulated as a nonlinear optimization problem taking into account the link scheduling, the transmission rates, and transmit power of all active TSs. The original nonlinear problem was converted into a convex optimization problem by employing an approximation of the SINR. We then derived the Lagrangian form of the convex optimization problem and employed the KKT optimality conditions [24] for deriving analytical expressions of the globally optimal transmit rate and power for our specific network topology. Finally, we obtained the maximum NL for both AWGN and Rayleigh fading channels. Our numerical results illustrated that fading has a detrimental impact on the achievable NL due to the poor channel conditions that require an increased transmit power to combat the effects of the fading. Furthermore, the simultaneous scheduling of links that interfere only weakly allowed us to take advantage of spatial reuse, where the activation of simultaneous transmissions at reduced rates necessitates reduced transmission power, which results in extending the NL. From this paper, we can conclude that the choice of scheduling depends on the application since a lower source rate favors infrequent transmissions requiring low transmit power, which do not suffer from interference, when aiming for extending the NL. However, for higher source rates, a higher NL can be achieved by aggressive spatial reuse.

Given the limitations of the centralized solution approach mentioned in Section III-B, the focus of this paper is on the information delay analysis. We also plan to extend our string topology model to a random network topology, where a single string (SN–DN pair) can be assumed to constitute a single route of the random topology. Nonetheless, conceiving distributed solutions for avoiding the limitations of our centralized scheme constitutes attractive future research directions.

References

[1] I. Dietrich and F. Dressler, "On the lifetime of wireless sensor networks," *ACM Trans. Sensor Netw.*, vol. 5, no. 1, pp. 5:1–5:39, Feb. 2009.

[2] W. Liu, K. Lu, J. Wang, G. Xing, and L. Huang, "Performance analysis of wireless sensor networks with mobile sinks," *IEEE Trans. Veh. Technol.*, vol. 61, no. 6, pp. 2777–2788, Jul. 2012.

[3] J. Chen, J. Li, and T. Lai, "Trapping mobile targets in wireless sensor networks: An energy-efficient perspective," *IEEE Trans. Veh. Technol.*, vol. 62, no. 7, pp. 3287–3300, Sep. 2013.

[4] M. Najimi, A. Ebrahimzadeh, S. Andargoli, and A. Fallahi, "Lifetime maximization in cognitive sensor networks based on the node selection," *IEEE Sensors J.*, vol. 14, no. 7, pp. 2376–2383, Jul. 2014.

[5] J. Du, K. Wang, H. Liu, and D. Guo, "Maximizing the lifetime of k-discrete barrier coverage using mobile sensors," *IEEE Sensors J.*, vol. 13, no. 12, pp. 4690–4701, Dec. 2013.

[6] H. Salarian, K. Chin, and F. Naghdy, "An energy-efficient mobile-sink path selection strategy for wireless sensor networks," *IEEE Trans. Veh. Technol.*, vol. 63, no. 5, pp. 2407–2419, Jun. 2014.

[7] J. W. Jung and M. Weitnauer, "On using cooperative routing for lifetime optimization of multi-hop wireless sensor networks: Analysis and guidelines," *IEEE Trans. Commun.*, vol. 61, no. 8, pp. 3413–3423, Aug. 2013.

[8] Y. Chen and Q. Zhao, "On the lifetime of wireless sensor networks," *IEEE Commun. Lett.*, vol. 9, no. 11, pp. 976–978, Nov. 2005.

[9] C. Cassandras, T. Wang, and S. Pourazarm, "Optimal routing and energy allocation for lifetime maximization of wireless sensor networks with nonideal batteries," *IEEE Trans. Control Netw. Syst.*, vol. 1, no. 1, pp. 86–98, Mar. 2014.

[10] D. Yuan, V. Angelakis, L. Chen, E. Karipidis, and E. Larsson, "On optimal link activation with interference cancelation in wireless networking," *IEEE Trans. Veh. Technol.*, vol. 62, no. 2, pp. 939–945, Feb. 2013.

[11] Z. Yang, Q. Zhang, and Z. Niu, "Throughput improvement by joint relay selection and link scheduling in relay-assisted cellular networks," *IEEE Trans. Veh. Technol.*, vol. 61, no. 6, pp. 2824–2835, Jul. 2012.

[12] R. Madan, S. Cui, S. Lall, and A. Goldsmith, "Cross-layer design for lifetime maximization in interference-limited wireless sensor networks," *IEEE Trans. Wireless Commun.*, vol. 5, no. 11, pp. 3142–3152, Nov. 2006.

[13] A. Goldsmith, *Wireless Communications*. Cambridge, U.K.: Cambridge Univ. Press, 2005.

[14] H. Yetgin, K. T. K. Cheung, and L. Hanzo, "Multi-objective routing optimization using evolutionary algorithms," in *Proc. IEEE WCNC*, Paris, France, Apr. 2012, pp. 3030–3034.

[15] L. Van Hoesel, T. Nieberg, J. Wu, and P. J. M. Havinga, "Prolonging the lifetime of wireless sensor networks by cross-layer interaction," *IEEE Wireless Commun. Mag.*, vol. 11, no. 6, pp. 78–86, Dec. 2004.

[16] H. Kwon, T. H. Kim, S. Choi, and B. G. Lee, "A cross-layer strategy for energy-efficient reliable delivery in wireless sensor networks," *IEEE Trans. Wireless Commun.*, vol. 5, no. 12, pp. 3689–3699, Dec. 2006.

[17] H. Nama, M. Chiang, and N. Mandayam, "Utility-lifetime trade-off in self-regulating wireless sensor networks: A cross-layer design approach," in *Proc. IEEE ICC*, Istanbul, Turkey, Jun. 2006, vol. 8, pp. 3511–3516.

[18] J. Zhu, S. Chen, B. Bensaou, and K.-L. Hung, "Tradeoff between lifetime and rate allocation in wireless sensor networks: A cross layer approach," in *Proc. 26th IEEE INFOCOM*, Anchorage, AK, USA, May 2007, pp. 267–275.

[19] S. Ehsan, B. Hamdaoui, and M. Guizani, "Radio and medium access contention aware routing for lifetime maximization in multichannel sensor networks," *IEEE Trans. Wireless Commun.*, vol. 11, no. 9, pp. 3058–3067, Sep. 2012.

[20] P. Li, S. Guo, and V. Leung, "Maximum-lifetime coding tree for multicast in lossy wireless networks," *IEEE Wireless Commun. Lett.*, vol. 2, no. 3, pp. 295–298, Jun. 2013.

[21] J.-H. Jeon, H.-J. Byun, and J.-T. Lim, "Joint contention and sleep control for lifetime maximization in wireless sensor networks," *IEEE Commun. Lett.*, vol. 17, no. 2, pp. 269–272, Feb. 2013.

[22] X. Liu, "A transmission scheme for wireless sensor networks using ant colony optimization with unconventional characteristics," *IEEE Commun. Lett.*, vol. 18, no. 7, pp. 1214–1217, Jul. 2014.

[23] H. Wang, N. Agoulmine, M. Ma, and Y. Jin, "Network lifetime optimization in wireless sensor networks," *IEEE J. Sel. Areas Commun.*, vol. 28, no. 7, pp. 1127–1137, Sep. 2010.

[24] S. P. Boyd and L. Vandenberghe, *Convex Optimization*. Cambridge, U.K.: Cambridge Univ. Press, 2004.

[25] A. Goldsmith and S.-G. Chua, "Variable-rate variable-power MQAM for fading channels," *IEEE Trans. Commun.*, vol. 45, no. 10, pp. 1218–1230, Oct. 1997.

[26] M. Albulet, *RF Power Amplifiers*. Raleigh, NC, USA: SciTech, 2001.

[27] D. Palomar and M. Chiang, "A tutorial on decomposition methods for network utility maximization," *IEEE J. Sel. Areas Commun.*, vol. 24, no. 8, pp. 1439–1451, Aug. 2006.

[28] K. Martinez, J. Hart, and R. Ong, "Environmental sensor networks," *Computer*, vol. 37, no. 8, pp. 50–56, Aug. 2004.

AUTHOR QUERIES

AUTHOR PLEASE ANSWER ALL QUERIES

AQ1 = Please provide keywords.

END OF ALL QUERIES

Correspondence

Cross-Layer Network Lifetime Maximization in Interference-Limited WSNs

Halil Yetgin, *Student Member, IEEE*,
Kent Tsz Kan Cheung, *Student Member, IEEE*,
Mohammed El-Hajjar, *Member, IEEE*, and
Lajos Hanzo, *Fellow, IEEE*

***Abstract*—In wireless sensor networks (WSNs), the network lifetime (NL) is a crucial metric since the sensor nodes usually rely on limited energy supply. In this paper, we consider the joint optimal design of the physical, medium access control (MAC), and network layers to maximize the NL of the energy-constrained WSN. The problem of NL maximization can be formulated as a nonlinear optimization problem encompassing the routing flow, link scheduling, transmission rate, and power allocation operations for all active time slots (TSs). The resultant nonconvex rate constraint is relaxed by employing an approximation of the signal-to-interference-plus-noise ratio (SINR), which transforms the problem to a convex one. Hence, the resultant dual problem may be solved to obtain the optimal solution to the relaxed problem with a zero duality gap. Therefore, the problem is formulated in its Lagrangian form, and the Karush–Kuhn–Tucker (KKT) optimality conditions are employed for deriving analytical expressions of the globally optimal transmission rate and power allocation variables for the network topology considered. The nonlinear Gauss–Seidel algorithm is adopted for iteratively updating the rate and power allocation variables using these expressions until convergence is attained. Furthermore, the gradient method is applied for updating the dual variables in each iteration. Using this approach, the maximum NL, the energy dissipation per node, the average transmission power per link, and the lifetime of all nodes in the network are evaluated for a given source rate and fixed link schedule under different channel conditions.**

***Index Terms*—Author, please supply index terms/keywords for your paper. To download the IEEE Taxonomy go to http://www.ieee.org/documents/taxonomy_v101.pdf.**

AQ1

NOMENCLATURE

- Number of nodes: $V = 10$.
- Total number of TSs per link: $N = 18$.
- Path-loss exponent: $m = 4$.
- Euclidean distance between consecutive nodes: $d[\mathrm{m}] = 1$.
- Maximum affordable transmit power per node: $(P_\upsilon)_{\max}[\mathrm{W}] = 50$.
- Spatially periodic link scheduling parameter: $T = \{3, 4, 5, 6, 7, 8, 9\}$.
- Initial battery energy per node: $E_\upsilon[\mathrm{J}] = 5000$.
- Spectral noise power density: $N0[\mathrm{dBm/Hz}] = 1$.
- Power amplifier inefficiency: $\alpha = 0.01$ [26].
- Set of all directed links: $\mathcal{L}$.
- A directed link spanning from transmitter i to receiver j: $l_{i,j}$.
- Set of all sensor nodes: $\mathcal{V}$.
- Network topology incidence matrix: $\mathbf{A}$.
- Emerging link of node υ: $l \in \mathcal{O}(\upsilon)$.
- Incoming link of node υ: $l \in \mathcal{I}(\upsilon)$.
- Network-channel-gain matrix: $\mathbf{G}$.
- Fading gain of the link between transmitter i and receiver j: $H_{i,j} = |h_{i,j}|^2$.
- NL: T_{net}.
- Reciprocal of NL: z.
- Transmission rate of link l in TS n: $r_{l,n}$.
- Transmit power of link l in TS n: $P_{l,n}$.
- Logarithm of the transmit power of link l in TS n: $Q_{l,n} = \log(P_{l,n})$.
- A set of dual variables for energy conservation constraint in (5): $\mathbf{\Omega}$.
- A set of dual variables for transmission rate constraint in (4): $\mathbf{\Psi}$.
- A set of dual variables for transmit power constraint in (6): $\boldsymbol{\vartheta}$.
- A set of dual variables for flow constraint in (3): $\boldsymbol{\mu}$.
- Convergence tolerance of the iterative algorithm: $\epsilon = 10^{-5}$.

I. INTRODUCTION

A wireless sensor network (WSN) is composed of a large number of nodes that monitor physical and environmental conditions and pass their accumulated data through the network to a sink node. There are numerous attractive applications for WSNs, including, for example, designing intelligent highways, controlling air pollution, providing remote health assistance for disabled or elderly people, monitoring river level variations, etc. Each of these applications may be composed of many sensor nodes, each of which consumes considerable amount of energy with sensing, communication, and data processing activities. Since each sensor node drains its limited energy supply as time elapses, the network lifetime (NL) is a crucial metric for these applications and has a major impact on the achievable performance of WSNs. Hence, we aim for analyzing and optimizing the NL of the WSNs under different channel conditions.

The NL defines the total amount of time during which the network is capable of maintaining its full functionality and/or achieves particular objectives during its operation, as exemplified in [1] and [2]. Specifically, the authors of [3]–[5] defined the expiration of the NL as the time instant at which a certain number of nodes in the network depleted their batteries. As a further example, the NL was defined in [6] as the lifetime of the specific sensor node associated with the highest energy consumption rate, whereas the authors of [7]–[9] considered the lifetime of the network to be expired at the particular instant, when the first node's battery was depleted. The NL in [8] was also defined as the instant when the first data collection failure occurred. In this paper, the NL is deemed to be expired, when at least one of the nodes fails due to its discharged battery. Therefore, extending the lifetime of a single node becomes an important and challenging task due to the battery-dependent characteristics of the wireless sensor nodes. This common NL definition is used in this paper since we consider

Manuscript received November 29, 2013; revised August 1, 2014; accepted September 20, 2014. This work was supported in part by the Republic of Turkey Ministry of National Education, by the Industrial Company Members of the Mobile VCE, by the U.K. Engineering and Physical Sciences Research Council, and by the Research Councils U.K. through the India–U.K. Advanced Technology Center of the European Union under the auspices of the Concerto Project and of the European Research Council's Senior Research Fellow Grant. The review of this paper was coordinated by Prof. S. Chen.

The authors are with the School of Electronics and Computer Science, University of Southampton, Southampton SO17 1BJ, U.K. (e-mail: hy3g09@ecs.soton.ac.uk; ktkc106@ecs.soton.ac.uk; meh@ecs.soton.ac.uk; lh@ecs.soton.ac.uk).

Color versions of one or more of the figures in this paper are available online at http://ieeexplore.ieee.org.

Digital Object Identifier 10.1109/TVT.2014.2360361

a network of linearly connected sensor nodes, where a single node's failure may destroy the entire string topology of nodes and, hence, the information of the source cannot be relayed to the sink. When considering the energy dissipated at a sensor node, the battery life is predominantly related to the node's communication activity, where the transmission rate and power must be optimized, while taking into account the battery capacity, the efficiency of the power amplifiers, the receiver and transmitter circuit energy consumption, and other physical layer parameters, including the modulation and coding schemes, the attainable coding gain, the path loss, and so on.

It is widely recognized that transmission at a high transmission rate requires the use of high transmit power, which potentially leads to strong interference among the transmission links [10]. Therefore, the battery depletion of an individual sensor node may become inevitable; hence, the NL may be reduced. However, in large networks, spatial reuse may be adopted for improving the attainable transmission rates at the cost of imposing interference on the network [11]. In this case, link scheduling [12] and multiple-access schemes [13] play a significant role in coordinating the resultant interference. More explicitly, we will demonstrate that scheduling weakly interfering links simultaneously allows the network to maintain a given sum rate at a reduced per-node transmit power, which hence extends the battery life of the nodes and the NL [10]. This is one of the methods routinely employed for taking advantage of spatial reuse to control the level of interference imposed on the network [11]. This method extends the NL since mitigating the interference imposed implies that each transmission requires less power. Therefore, intelligent scheduling should carefully balance the number of simultaneous active links and their transmission duration to keep the required transmit power at a minimum. Furthermore, multihop relaying [14] is capable of conserving the energy of the source node (SN) since intermediate nodes may be employed for reducing the transmission power necessary for maintaining a given end-to-end rate. Hence, we consider the joint optimal design of the transmission rate, transmission power, and scheduling to maximize the NL of energy-constrained WSNs.

There is a paucity of contributions in the literature on the issue of cross-layer NL optimization in the context of WSNs. Hoesel *et al.* [15] proposed a cross-layer approach for jointly optimizing the medium access control (MAC) and routing layer to maximize the NL. Chen and Zhao [8] proposed an efficient MAC protocol that relies both on the channel state information and on the MAC's knowledge of the residual energy to maximize the NL. In [16], Kwon *et al.* investigated the NL maximization problem of WSNs, which jointly considers the physical layer, the MAC layer, and the routing layer in conjunction with the transmission success probability constraint. Additionally, the tradeoff between NL maximization and application performance was studied in [17] by using cross-layer optimization. A similar study also investigated the tradeoff between the energy consumption and application-layer performance with the aid of cross-layer optimization of WSNs [18]. Another cross-layer approach conceived for maximizing the NL was proposed in [19], where MAC-aware routing optimization schemes were designed for WSNs that are capable of multichannel access. In [20], Li *et al.* invoked random linear network coding for the lifetime maximization of wireless networks within a fixed-rate system for communicating over both additive white Gaussian noise (AWGN) and Rayleigh fading channels. A different approach to NL maximization was introduced in [21], where both contention and sleep control probabilities of the sensor nodes were utilized for formulating the NL maximization problem, while guaranteeing both the required throughput and the signal-to-interference-plus-noise ratio (SINR) requirements. Najimi *et al.* [4] proposed a node selection algorithm for balancing the energy usage of the sensors in a fixed-mode cognitive sensor network. A similar idea

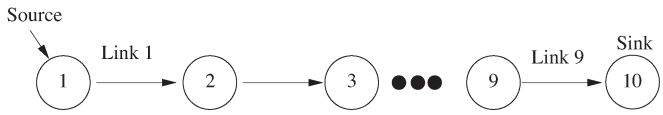

Fig. 1. String topology with $V = 10$ nodes, including an SN and a DN.

to that of the optimal control approach invoked for maximizing the NL with the aid of a carefully selected routing probability was exploited in [9], where all the sensors were configured to deplete their energy exactly at the same time for lifetime maximization. Another similar study advocating an effective transmission scheme was proposed in [22], where both the maximum possible energy efficiency and the best possible energy balancing were maintained with the aid of ant colony optimization.

However, all related work aforementioned considers either non-adaptive, i.e., fixed-mode system, or nonfading channel characteristics. An adaptive system conceived for NL maximization was studied by Wang *et al.* [23], who considered only an interference-free scenario for an AWGN channel by employing the Karush–Kuhn–Tucker (KKT) optimality conditions [24] to the optimal time-division multiple-access (TDMA) NL maximization problem of [12] to derive the analytical expressions of the optimal NL. Madan *et al.* [12] considered an interference-limited scenario relying on an adaptive system, operating in an AWGN channel, but the impact of the fading channel characteristics on the NL was not presented. Wang *et al.* [23] obtained a closed-form solution for a specific network topology. By contrast, a generalized string network topology consisting of an arbitrary number of nodes is considered in our treatise, where we employ the KKT optimality conditions for obtaining the optimal solution to the NL maximization problem using closed-form expressions. Therefore, we are able to derive analytical expressions of the globally optimal NL for a string network operating in an interference-limited scenario, while communicating either over an AWGN or over fading channels for a given link schedule. Furthermore, the maximum NL, the energy dissipation per node, the average transmission power per link, and the lifetime of all nodes in the network may be obtained. We quantify how the maximum NL decreases as a function of the fading statistics due to the poor channel conditions. Furthermore, it is demonstrated that given a certain network sum rate, the simultaneous scheduling of weakly interfering links benefits from the associated spatial reuse by allowing each node to transmit at a lower rate, which requires a reduced transmission power and hence results in a higher NL. Against this backdrop, the novel contributions of this paper can be summarized as follows.

1) The KKT optimality conditions [24] are invoked for deriving the analytical expressions of the globally optimal NL for an interference-limited string topology.
2) In addition to the line-of-sight (LOS) AWGN channel model, the non-LOS Rayleigh block-fading channel model is adopted for studying the effects of fading on the NL.
3) The maximum NL is evaluated, and the energy dissipation per node, the average transmission power per link, and the lifetime of all nodes in the network are quantified for a given link schedule and source rate in both LOS AWGN and non-LOS Rayleigh block-fading channels.
4) The substantial effect of the distance among the consecutive nodes on the NL is also analyzed for lower source rates, when operating in a Rayleigh fading channel. The impact of the interferers is also investigated in the context of higher source rates.

The remainder of this paper is organized as follows. Section II describes our system model and the constraints of the optimization problem considered. Our problem formulation and solution approach

Links \ Slots	1	2	3	4	5	6	7	8	9	10	11	12	13	14	15	16	17	18
l_{1-2}	●+			●			●			●+			●			●		
l_{2-3}		●+			●			●			●+			●			●	
l_{3-4}			●+			●			●			●+			●			●
l_{4-5}	●			●+			●			●			●+			●		
l_{5-6}		●			●+			●			●			●+			●	
l_{6-7}			●			●+			●			●			●+			●
l_{7-8}	●			●			●+			●			●			●+		
l_{8-9}		●			●			●+			●			●			●+	
l_{9-10}			●			●			●+			●			●			●+

●: T=3 spatially periodic link schedule +: T=9 spatially periodic link schedule

Fig. 2. Spatially periodic link schedule with time sharing parameter $T = 3$ and $T = 9$ when $N = 18$ and $V = 10$.

are presented in Section III, and our numerical results are shown in Section IV. Our conclusions are provided in Section V.

II. System Model

Here, we first describe the network model,[1] which relies on a string topology.[2] Second, we detail our transceiver model in Section II-B, where we evaluate the NL for transmission over both AWGN and block-fading channels. Moreover, our transmission scheduling strategy is also described and exemplified at the end of Section II-B.

A. Network Model

We consider a string topology composed of V sensor nodes, where the SN and the destination node (DN) are linearly connected by intermediate nodes. An example of this string topology for $V = 10$ is shown in Fig. 1; hence, the number of links is $L = V - 1 = 9$.

Each link is unidirectional, and the antenna of each node is omnidirectional. The network can be modeled as a directed graph $\mathcal{G} = \{\mathcal{V}, \mathcal{L}\}$, where $\mathcal{V} = \{1, 2, 3, \ldots, V\}$ is the set of all sensor nodes, and $\mathcal{L} = \{l_{1,2}, l_{2,3}, \ldots, l_{V-1,V}\}$ is the set of all directed links in the network. Here, $l_{i,j}$ represents the directed link spanning from the transmitter node i to receiver node j. Therefore, the topology can be modeled with the aid of an incidence matrix of the graph $\mathcal{G}$ given by $\mathbf{A} \in \mathbf{R}^{|\mathcal{V}|\times|\mathcal{L}|}$. The entries $a_{v,l}$ of $\mathbf{A}$ are given by

$$a_{v,l} = \begin{cases} 1, & \text{if } v \text{ is the transmitter of link } l \\ -1, & \text{if } v \text{ is the receiver of link } l \\ 0, & \text{otherwise.} \end{cases} \quad (1)$$

We consider a single commodity flow. Therefore, by the conservation of flow, the constraint $\sum_{l\in\mathcal{O}(v)}(\sum_{n=1}^{N} r_{l,n}) = \sum_{l\in\mathcal{I}(v)} \times (\sum_{n=1}^{N} r_{l,n})$ may be written for each node v in the absence of an external source or sink, where N is the total number of time slots (TSs) per TDMA frame, and $r_{l,n}$ is the transmission rate of link l in TS n. Additionally, $l \in \mathcal{O}(v)$ denotes the emerging link, and $l \in \mathcal{I}(v)$ represents the incoming link of node v.

[1]Our network model is a centralized one, where the sink node is assumed to be a control center.

[2]A string topology is chosen since, in this simple scenario, the effect of transmission variables on the NL can be explicitly exposed and analyzed. Our string topology scenario is also capable of providing insights concerning a randomly distributed network with many nodes since a specific set of nodes can be assumed to constitute a single route of the randomly distributed network.

B. Channel Model and MAC Layer Scheme

In each TS n, each node can only act as a transmitter or a receiver. Each transmitter is only allowed to communicate with a single receiver, which cannot receive from other nodes in the same TS. This is due to the half-duplex nature of the transceivers, where nodes communicate on the same shared wireless channel. The channel gain of the link between transmitter i and receiver j is given by $G_{i,j} = 1/(d_{i,j})^m$, where $d_{i,j}$ is the distance between nodes i and j, whereas the path-loss exponent is $m = 4$. These channel gains are arranged into a network-channel-gain matrix denoted by $\mathbf{G}$. Each node v is capable of transmitting at a power less than the maximum power of that node denoted by $(P_v)_{\max}$. The total energy dissipation at a node cannot exceed the initial battery energy of that node. No node is allowed to simultaneously transmit multiple data packets, and the link quality is defined by the SINR.

The LOS AWGN channel is modeled by a certain propagation path-loss law and a fixed noise power at the receivers. Given a specific link l, the SINR is denoted by Γ_l in the AWGN channel model. The maximum achievable rate per unit bandwidth is $r_l = \log(1 + K \cdot \Gamma_l)$ given in nats/s/Hz, where $K = -1.5/\log(5\text{BER})$ [25], and BER represents the target bit error ratio (BER) required by the system. Therefore, the SINR is given by [13] $\Gamma_{l_{i,j},n} = G_{i,j}P_{i,n}/(\sum_{i'\neq i} G_{i',j}P_{i',n} + N_0)$, where $P_{i,n}$ is the transmission power of node i in TS n. Furthermore, K is assumed to incorporate the coding gain and any other gain factors, which is a suitable model for M-ary quadrature amplitude modulation (MQAM) associated with $M \geq 4$ [25]. The factor K is assumed absorbed into the gain matrix $\mathbf{G}$.

On the other hand, when considering fading channels, the channel of each link is modeled as a multiplicative Rayleigh fading channel contaminated by the noise added at the receivers. We consider block fading or quasi-static fading, where the fading gain is kept constant throughout the TDMA frame for the link, which represents slowly fading channels, i.e., low Doppler pedestrian speeds. This requires a modification of the SINR used in AWGN channels, which is formulated as [25] $\widetilde{\Gamma}_{l_{i,j},n} = H_{i,j}G_{i,j}P_{i,n}/(\sum_{i'\neq i} H_{i',j}G_{i',j}P_{i',n} + N_0)$, where $H_{i,j} = |h_{i,j}|^2$ is the fading gain of the link between transmitter i and receiver j.

We assume a link scheduling associated with spatially periodic time sharing [12], where we consider a distance T between links that are transmitting in the same TS, and the link is reactivated after every T TSs. Fig. 2 shows the spatially periodic link scheduling for $T=3$ and $T=9$. For $T=3$, at the first TS, links $l_{1,2}, l_{4,5}, l_{7,8}$ are simultaneously scheduled, and each link is activated six times in total in TSs of 1, 4, 7, 10, 13, and 16. On the other hand, for $T=9$, each TS has only a single active transmission, and each link is activated twice, as shown in Fig. 2.

III. Problem Formulation and Solution

Having discussed the assumptions and constraints in Section II, the NL maximization problem [12] can be formulated as in

$$\min. \quad z \tag{2}$$

$$\text{s.t.} \quad \mathbf{A}(\mathbf{r}_1+\mathbf{r}_2+\cdots+\mathbf{r}_N)=\mathbf{s}\cdot N \tag{3}$$

$$\left(\frac{N_0}{G_{i,j}}\cdot e^{r_{l_{i,j},n}-Q_{l_{i,j},n}} + \sum_{l_{i',j'}\in\mathcal{L}_n, i'\neq i}\frac{G_{i',j}}{G_{i,j}}\cdot e^{r_{l_{i,j},n}+Q_{l_{i',j',n}}-Q_{l_{i,j},n}}\right) - 1 \leq 0 \quad \forall n,\ l\in\mathcal{L}_n \tag{4}$$

$$\sum_{n=1}^{N}\left(\sum_{l\in\mathcal{O}(v)\cap\mathcal{L}_n}\left((1+\alpha)\cdot e^{Q_{l_{i,j},n}}+P_{\text{ct}}\right) + \sum_{l\in\mathcal{I}(v)\cap\mathcal{L}_n}P_{\text{cr}}\right)\leq z\cdot E_v\cdot N \quad \forall v \tag{5}$$

$$Q_{l_{i,j},n}\leq\log((P_i)_{\max}),\ l\in\mathcal{L}_n \tag{6}$$

$$\mathbf{r}_n\geq 0 \quad \forall n \tag{7}$$

$$r_{l_{i,j},n}=0 \quad \forall l\notin\mathcal{L}_n \tag{8}$$

where (4) has been modified, so that it constitutes a strictly convex constraint. See the Nomenclature list on the first page of this paper for the specific parameters utilized in our simulations.

The links that are active in TS n are denoted by the set $\mathcal{L}_n$, and $\mathbf{s}=[s_1,0,\ldots,-s_1]^T$ is the source rate vector, where the first and last elements are nonzero but the remaining elements are set to zero because the first node is the SN and the last node is the DN, and the other nodes act as relay nodes (RN). The variables of the optimization problem are z, $Q_{l,n}$, and $r_{l,n}$, for $l\in\mathcal{L}_n$, $n=1,\ldots,N$. The vector of rate variables associated with TS n is given by $\mathbf{r}_n=[r_{l_{1,2},n}, r_{l_{2,3},n},\ldots,r_{l_{V-1,V},n}]^T$. Assuming that the transmitter and receiver circuits do not dissipate energy, we can set $P_{\text{ct}}=0$ and $P_{\text{cr}}=0$, where P_{ct} and P_{cr} denote the power required by the transmitter and receiver circuits, respectively. Furthermore, we denote the power amplifier inefficiency as α [26]. The lifetime of a node in the network is denoted by T_v, which corresponds to the time during which the node runs out of battery. The NL is defined as the time during which at least one node completely drains its battery, i.e., we have $T_{\text{net}}=\min_{v\neq V, v\in\mathcal{V}}. T_v$. The objective function (OF) and the constraints of the optimization problem are as follows.

1) *Objective function—Minimization of reciprocal of the NL*: In (2), we minimize z so that the NL is maximized. Here, we used a minimization technique in our problem. We can rewrite (5) as $\sum_{n=1}^{N}(\sum_{l\in\mathcal{O}(v)\cap\mathcal{L}_n}((1+\alpha)\cdot e^{Q_{l_{i,j},n}}+P_{\text{ct}})+\sum_{l\in\mathcal{I}(v)\cap\mathcal{L}_n}P_{\text{cr}})\leq(1/T_{\text{net}})\cdot E_v\cdot N$, and we can multiply the left-hand side of the inequality by T_{net}, but the multiplication of the two optimization variables is in general nonconvex. Therefore, we use a change of variable and minimize $z=1/T_{\text{net}}$, which keeps the right-hand side of the inequality linear and left-hand side convex.
2) *Flow conservation constraint*: In (3), using matrix $\mathbf{A}$ with entries given by 1 ensures that flow conservation is preserved, and physically, this means that the information generated at the SN has to arrive at the DN.
3) *Transmission rate constraint*: We have to satisfy the rate constraint of our interference-limited scenario for each link of the same TS in (4).
4) *Energy conservation constraint*: Each sensor node can dissipate at most the initial amount of battery energy, which we set to 5000 J. Therefore, in (5), the energy conservation constraint is given for each node.
5) *Transmit power constraint*: Equation (6) represents the transmission power at a node, which has to be less than the maximum affordable transmit power of that node.
6) *No transmission*: Finally, the transmission rate of nodes that are not scheduled for transmission is set to zero in (8).

The optimization problem is solved for the sake of finding the optimal scheme for transmission over each link for a given link schedule, which is defined by the spatially periodic time sharing discussed in Section II-B. However, to obtain the globally optimal solutions, we wish to show that (2)–(8) represent a convex optimization problem, composed of a convex OF, convex inequality constraint functions, and affine equality constraint functions. It is clear that (3) and (8) are affine, (2) and (5)–(7) are convex, and (4) is strictly convex [24]. Therefore, (2)–(8) define a strictly convex optimization problem that has a unique solution. We can convert the problem into its Lagrangian form and rely on the KKT optimality conditions [24] for deriving the analytical expressions of the globally optimal transmission scheme for the string network topology of Fig. 1.

A. Karush–Kuhn–Tucker Optimality Conditions

Lets us define the sets of the optimization variables and of the Lagrangian multipliers as $\boldsymbol{R}=\{r_{l_{1,2},1},\ldots,r_{l_{V-1,V},N}\}$, $\boldsymbol{Q}=\{Q_{l_{1,2},1},\ldots,Q_{l_{V-1,V},N}\}$, $\boldsymbol{\mu}=\{\mu_1,\ldots,\mu_V\}$, $\boldsymbol{\Psi}=\{\psi_{l_{1,2},1},\ldots,\psi_{l_{V-1,V},N}\}$, $\boldsymbol{\Omega}=\{\omega_1,\ldots,\omega_{V-1}\}$, and $\boldsymbol{\vartheta}=\{\vartheta_{l_{1,2},1},\ldots,\vartheta_{l_{V-1,V},N}\}$. Thus, the partial Lagrangian of (2)–(8) is given by (9), shown at the bottom of the next page, where ω_v, $\psi_{l_{i,j},n}$, and $\vartheta_{l_{i,j},n}$, μ_v are the dual variables associated with the constraints (3)–(6), respectively. Constraints (7) and (8) are taken into account, when deriving the optimal primal variables.

The KKT conditions for (9) are given by (10)–(16), shown at the bottom of the next page, where $\mathcal{I}^{-1}(l)$ denotes the node associated with the incoming link l, and $\mathcal{O}^{-1}(l)$ represents the node associated with the outgoing link l. Since the primal problem is convex, if $z,\boldsymbol{R},\boldsymbol{Q},\boldsymbol{\Omega},\boldsymbol{\Psi},\boldsymbol{\vartheta},\boldsymbol{\mu}$ represent arbitrary points that satisfy the KKT optimality conditions given by the primal feasibility in (3)–(6), the dual feasibility of (16), the complementary slackness in (13)–(15), and the first-order optimality in (10)–(12), then $z,\boldsymbol{R},\boldsymbol{Q}$ are primal optimal, and $\boldsymbol{\Omega},\boldsymbol{\Psi},\boldsymbol{\vartheta},\boldsymbol{\mu}$ are dual optimal[3] with zero duality gap[4] [24].

[3]Optimal solution of the primal (original) problem is expressed as primal optimal and the dual problem provides us a lower bound on the optimal value of the original optimization problem. Hence, the dual optimal is a lower bound on the primal optimal.

[4]The duality gap is defined as the difference between the optimal primal and optimal dual solutions.

B. Problem Solution

From (11) and (12), the optimal values of $\boldsymbol{Q}$ and $\boldsymbol{R}$ in iteration $(t+1)$ are given by (17) and (18), respectively, shown at the bottom of the next page. Note that, due to the interference terms in (11) and (12), each optimal variable in $\boldsymbol{Q}$ and $\boldsymbol{R}$ is dependent on the other variables of $\boldsymbol{Q}$ and $\boldsymbol{R}$, which implies that they are interdependent, hence requiring a centralized solution approach.[5] Therefore, the Gauss–Seidel algorithm [27] is utilized for iteratively updating these variables in a circular fashion.

The dual OF is defined as the minimum value of the Lagrangian (9) over $z, \boldsymbol{R}, \boldsymbol{Q}$ given by $g(\boldsymbol{\Omega}, \boldsymbol{\Psi}, \boldsymbol{\vartheta}, \boldsymbol{\mu}) = \inf_{z,\boldsymbol{R},\boldsymbol{Q}} \mathcal{L}(z, \boldsymbol{R}, \boldsymbol{Q}, \boldsymbol{\Omega}, \boldsymbol{\Psi}, \boldsymbol{\vartheta}, \boldsymbol{\mu})$, which is a linear problem even if the primal problem is nonconvex. The dual function $g(\boldsymbol{\Omega}, \boldsymbol{\Psi}, \boldsymbol{\vartheta}, \boldsymbol{\mu})$ may be maximized to find a lower bound for the optimal value of the primal problem. Then, we can write the dual problem as follows:

$$\max_{\boldsymbol{\Omega},\boldsymbol{\Psi},\boldsymbol{\vartheta},\boldsymbol{\mu}} \quad g(\boldsymbol{\Omega}, \boldsymbol{\Psi}, \boldsymbol{\vartheta}, \boldsymbol{\mu})$$
$$\text{s.t.} \quad \boldsymbol{\Omega} \geq 0,\ \boldsymbol{\Psi} \geq 0,\ \boldsymbol{\vartheta} \geq 0$$

which is a linear optimization problem. When the primal problem is convex, this lower bound is tight; therefore, the duality gap is zero. Since the dual problem is continuously differentiable, the gradient ascent algorithm [27] is utilized to solve the maximization problem by simply evaluating a series of closed-form expressions. The gradient

[5]The calculation of both the transmit power and of the rate of a specific node relies on the prior knowledge gleaned from other nodes, possibly from its interferers. Therefore, a control center is required, which handles the variables of the optimization problem and passes the near-instantaneous values of the variables to each of the individual nodes. Compared with a distributed scheme, this centralized solution will impose delay on the system since operations such as channel estimation are required at the initial stage. The near-instantaneous transmission rate and power values computed by the control center constituted by the sink node should be forwarded to each individual node. Therefore, a nonnegligible delay will be imposed on the reception of the sink node.

$$\begin{aligned}\mathcal{L}(z, \boldsymbol{R}, \boldsymbol{Q}, \boldsymbol{\Omega}, \boldsymbol{\Psi}, \boldsymbol{\vartheta}, \boldsymbol{\mu}) = z &+ \sum_{v=1}^{V-1} \omega_v \cdot \left[\sum_{n=1}^{N} \left(\sum_{l \in \mathcal{O}(v) \cap \mathcal{L}_n} \left((1+\alpha) \cdot e^{Q_{l_{i,j},n}} \right) \right) - z \cdot E_v \cdot N \right] \\ &+ \sum_{n=1}^{N} \sum_{l \in \mathcal{L}_n} \psi_{l_{i,j},n} \cdot \left[\left(\frac{N_0}{G_{i,j}} e^{r_{l_{i,j},n} - Q_{l_{i,j},n}} + \sum_{l_{i',j'} \in \mathcal{L}_n, i' \neq i} \frac{G_{i',j}}{G_{i,j}} e^{r_{l_{i,j},n} + Q_{l_{i',j'},n} - Q_{l_{i,j},n}} \right) - 1 \right] \\ &+ \sum_{n=1}^{N} \sum_{l \in \mathcal{L}_n} \vartheta_{l_{i,j},n} \cdot \left[Q_{l_{i,j},n} - \log\left((P_i)_{\max} \right) \right] + \sum_{v=1}^{V} \mu_v \cdot \left[\sum_{l \in \mathcal{I}(v)} \left(\sum_{n=1}^{N} r_{l_{i,j},n} \right) - \sum_{l \in \mathcal{O}(v)} \left(\sum_{n=1}^{N} r_{l_{i,j},n} \right) \right] \end{aligned} \tag{9}$$

$$\frac{\partial \mathcal{L}}{\partial z} = 1 - \sum_{v=1}^{V} \omega_v (E_v \cdot N) = 0 \tag{10}$$

$$\frac{\partial \mathcal{L}}{\partial r_{l_{i,j},n}} = \mu_{\mathcal{I}^{-1}(l)} - \mu_{\mathcal{O}^{-1}(l)} + \psi_{l_{i,j},n} \left(\frac{N_0}{G_{i,j}} e^{r_{l_{i,j},n} - Q_{l_{i,j},n}} + \sum_{l_{i',j'} \in \mathcal{L}_n, i' \neq i} \frac{G_{i',j}}{G_{i,j}} e^{r_{l_{i,j},n} + Q_{l_{i',j'},n} - Q_{l_{i,j},n}} \right) = 0 \quad \forall l, n \tag{11}$$

$$\begin{aligned}\frac{\partial \mathcal{L}}{\partial Q_{l_{i,j},n}} = &\omega_{\mathcal{O}^{-1}(l)} \left((1+\alpha) e^{Q_{l_{i,j},n}} \right) + \vartheta_{l_{i,j},n} \\ &- \psi_{l_{i,j},n} \left(\frac{N_0}{G_{i,j}} e^{r_{l_{i,j},n} - Q_{l_{i,j},n}} + \sum_{l_{i',j'} \in \mathcal{L}_n, i' \neq i} \frac{G_{i',j}}{G_{i,j}} e^{r_{l_{i,j},n} + Q_{l_{i',j'},n} - Q_{l_{i,j},n}} \right) = 0 \quad \forall l, n \end{aligned} \tag{12}$$

$$0 = \sum_{v=1}^{V-1} \omega_v \cdot \left[\sum_{n=1}^{N} \left(\sum_{l \in \mathcal{O}(v) \cap \mathcal{L}_n} \left((1+\alpha) e^{Q_{l_{i,j},n}} \right) \right) - z \cdot E_v \cdot N \right] \tag{13}$$

$$0 = \psi_{l_{i,j},n} \cdot \left[\left(\frac{N_0}{G_{i,j}} e^{r_{l_{i,j},n} - Q_{l_{i,j},n}} + \sum_{l_{i',j'} \in \mathcal{L}_n, i' \neq i} \frac{G_{i',j}}{G_{i,j}} e^{r_{l_{i,j},n} + Q_{l_{i',j'},n} - Q_{l_{i,j},n}} \right) - 1 \right] \quad \forall l, n \tag{14}$$

$$0 = \vartheta_{l_{i,j},n} \cdot \left[Q_{l_{i,j},n} - \log\left((P_i)_{\max} \right) \right] \quad \forall l, n \tag{15}$$

$$\omega_v \geq 0,\ \psi_{l_{i,j},n} \geq 0,\ \vartheta_{l_{i,j},n} \geq 0 \tag{16}$$

of the Lagrangian function defines the search directions at the current point. Each dual variable is incremented in the direction of the positive gradient in (19)–(22), shown at the bottom of the page, where t is the iteration index, and $[\cdot]^+$ denotes $\max(0,\cdot)$. Provided that $\Delta_{\boldsymbol{\Omega}} > 0$, $\Delta_{\boldsymbol{\Psi}} > 0$, $\Delta_{\boldsymbol{\vartheta}} > 0$, and $\Delta_{\boldsymbol{\mu}} > 0$ are sufficiently small positive step sizes, the dual variables $\boldsymbol{\Omega}^t$, $\boldsymbol{\Psi}^t$, $\boldsymbol{\vartheta}^t$, and $\boldsymbol{\mu}^t$ converge to the dual optimal variables $\boldsymbol{\Omega}^*$, $\boldsymbol{\Psi}^*$, $\boldsymbol{\vartheta}^*$, and $\boldsymbol{\mu}^*$, respectively, as $t \to \infty$. In our case, the optimization problem shown in (2)–(8) is strictly convex; thus, the duality gap is zero, and the solution is unique.

IV. Experimental Results

In our experiments, we use the parameters of $d = 1$ m, $\alpha = 0.01$ [26], $K = 1$, $N_0 = 1$ dBm/Hz, $E_v = 5000$ J[6], $(P_i)_{\max} = 50$ W, $N = 18$, $s_1 = \{0.2, 0.3, 0.4, 0.5, 0.6, 0.7\}$ nats/s/Hz $\approx \{0.29, 0.43, 0.58, 0.72, 0.87, 1.01\}$ bits/s/Hz, $T = \{3, 4, 5, 6, 7, 8, 9\}$, convergence tolerance of iterative algorithm $\epsilon = 10^{-5}$.

Fig. 3 shows the NL versus source rate trends for a fixed link schedule and for various spatially periodic time sharing parameters T, where the channel in each link is a LOS AWGN channel characterized by fixed noise power. As expected, the NL decays as a function of the source rate, as shown in Fig. 3. This is because a higher source rate requires a higher transmission rate and, hence, higher transmission power. Furthermore, in our model, the weakly interfering nodes are scheduled to transmit simultaneously; hence, each link becomes capable of transmitting at a lower rate, while still satisfying all the transmit requirements of the SN. This necessitates lower transmission power. Using the $T = 9$ spatially periodic time schedule of Fig. 2 corresponds to a TDMA scheme since there is only a single transmission in each TS, as shown in Fig. 2. However, since the time frame of Fig. 2 consists of 18 TSs, a specific link is scheduled to transmit twice during the whole time frame. Despite the fact that the $T = 9$ link schedule does not impose any interference, it results in the lowest NL according to Fig. 3. Although interference is present in

[6]For example, this is the energy storage capacity of an AAA alkaline long-life battery.

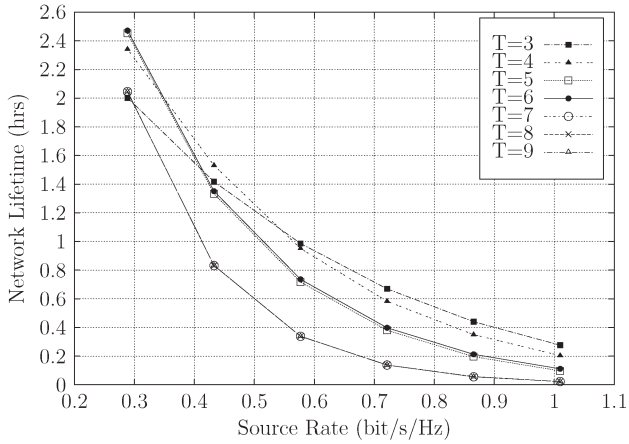

Fig. 3. Network lifetime for different spatially periodic schedules and source rates in the AWGN channel.

$$Q_{l_{i,j},n}^{t+1} = \log\left[\left(\mu_i^t - \mu_j^t - \vartheta_{l_{i,j},n}^t\right)\cdot\left(\omega_i^t(1+\alpha) + \sum_{l_{i',j'}\in\mathcal{L}_n, l_{i',j'}\neq l_{i,j}, i'\geq i} \psi_{l_{i',j'},n}^t\left(\frac{G_{i,j'}}{G_{i',j'}}\cdot e^{r_{l_{i',j'},n}^t - Q_{l_{i',j'},n}^t}\right)\right.\right.$$
$$\left.\left. + \sum_{l_{i',j'}\in\mathcal{L}_n, l_{i',j'}\neq l_{i,j}, i'<i} \psi_{l_{i',j'},n}^t\left(\frac{G_{i,j'}}{G_{i',j'}}\cdot e^{r_{l_{i',j'},n}^t - Q_{l_{i',j'},n}^{t+1}}\right)\right)^{-1}\right] \quad \forall l,n \tag{17}$$

$$r_{l_{i,j},n}^{t+1} = \log\left[\frac{\mu_i^t - \mu_j^t}{\psi_{l_{i,j},n}^t\cdot\left(\frac{N_0}{G_{i,j}} + \sum_{l_{i',j'}\in\mathcal{L}_n, l_{i',j'}\neq l_{i,j}} \frac{G_{i',j}}{G_{i,j}}\cdot e^{Q_{l_{i',j'},n}^{t+1}}\right)}\right] + Q_{l_{i,j},n}^{t+1} \quad \forall l,n \tag{18}$$

$$\omega^{t+1} = \left[\omega^t + \Delta_\omega\left(\sum_{n=1}^{N}\left(\sum_{l\in\mathcal{O}(v)\cap\mathcal{L}_n}\left((1+\alpha)\cdot e^{Q_{l_{i,j},n}}\right)\right) - z\cdot E_v\cdot N\right)\right]^+ \tag{19}$$

$$\psi^{t+1} = \left[\psi^t + \Delta_\psi\left(\left(\frac{N_0}{G_{i,j}}e^{r_{l_{i,j},n} - Q_{l_{i,j},n}} + \sum_{l_{i',j'}\in\mathcal{L}_n, i'\neq i}\frac{G_{i',j}}{G_{i,j}}e^{r_{l_{i,j},n} + Q_{l_{i',j'},n} - Q_{l_{i,j},n}}\right) - 1\right)\right]^+ \tag{20}$$

$$\vartheta^{t+1} = \left[\vartheta^t + \Delta_\vartheta(Q_{l_{i,j},n} - \log((P_i)_{\max}))\right]^+ \tag{21}$$

$$\mu^{t+1} = \left[\mu^t + \Delta_\mu\left(\sum_{l\in\mathcal{I}(v)}\left(\sum_{n=1}^{N} r_{l_{i,j},n}\right) - \sum_{l\in\mathcal{O}(v)}\left(\sum_{n=1}^{N} r_{l_{i,j},n}\right)\right)\right] \tag{22}$$

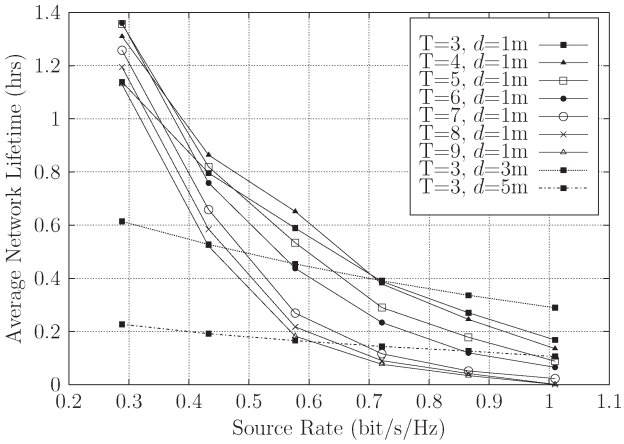

Fig. 4. Network lifetime for different spatially periodic schedules and source rates in a block-fading channel.

the $T = 3$ scenario since each link can be activated three times more often than in the $T = 9$ scenario, each link in the $T = 3$ scenario can be activated at lower transmission power, while still satisfying the end-to-end rate constraint. Therefore, the spatial reuse assisted us in the $T = 3$ scenario for increasing the NL. We can follow Fig. 2 to find out how many transmissions there are per link for a given value of T. For example, the $T = 3$ schedule allows a link to be scheduled six times, which requires a reduced transmission rate, since the total source rate that is delivered over different TSs is using six transmissions. From the flow conservation equality constraint of the optimization problem seen in (3), we have $\mathbf{A}(\mathbf{r}_1 + \mathbf{r}_2 + \cdots + \mathbf{r}_N) = \mathbf{s} \cdot N$. For example, let us assume that the source rate equals to 0.29 bits/s/Hz. Then, we obtain $18 \cdot 0.29 = 5.22$ bits/s/Hz, which has to be divided into six transmissions, corresponding to a 0.87 bits/s/Hz per link transmission rate for $T = 3$. However, when we have $T = 9$, we obtain a 2.61-bits/s/Hz per link transmission rate since a link is only activated twice during the whole time frame. Therefore, the transmission rate per link converges to 0.87 bits/s/Hz for $T = 3$ and 2.61 bits/s/Hz for $T = 9$. Hence, $T = 9$ requires three times as much transmission power as $T = 3$. The required transmit power in weakly interfering links is quite low compared with that for $T = 9$, which is the scenario requiring the highest transmission rate. Hence, again, we surmise that simultaneous scheduling benefits from reduced transmission power due to its reduced transmission rate per link. This is because the spatially periodic schedule allows us to schedule more transmissions during the same TS or to activate the same link more than once in different TSs. This explains the steep decay of the NL for $T = 9$.

When considering the effects of node density on a given fixed link schedule, we expect a network supporting less than $V = 10$ nodes to be exposed to less interference. Therefore, the transmission power of each link can be reduced without reducing the end-to-end transmission rate, which results in a higher NL. On the other hand, upon increasing the node density, we expect the NL to decrease since more interferers are introduced, but the same transmission rate is required.

Fig. 4 represents the NL versus source rate tradeoff for a fixed link schedule and for various spatially periodic time sharing parameter values of T when each link obeys an independent and identically distributed Rayleigh block-fading channel. Naturally, the NL was reduced compared with the results of Fig. 3 recorded for an AWGN channel due to requiring higher transmit power to combat the effects of fading. We also analyzed the impact of the internode distance on the NL for the $T = 3$-based link schedule, when communicating over a Rayleigh fading channel, as shown in Fig. 4. Increasing the distance between the consecutive nodes substantially reduced the NL, particularly for lower source rates. However, quite surprisingly, increasing the distance between the consecutive nodes from 1 to 3 m resulted in an improved NL for higher source rates. This is due to the reduced impact of the interferers located at a higher distance. More explicitly, although the transmit power required had to be increased to satisfy the rate constraint, at the same time the interferers were moved a bit further away. Therefore, the total energy dissipation of the $d = 3$ m scenario is still lower than that of the $d = 1$ m scenario associated with higher source rates.

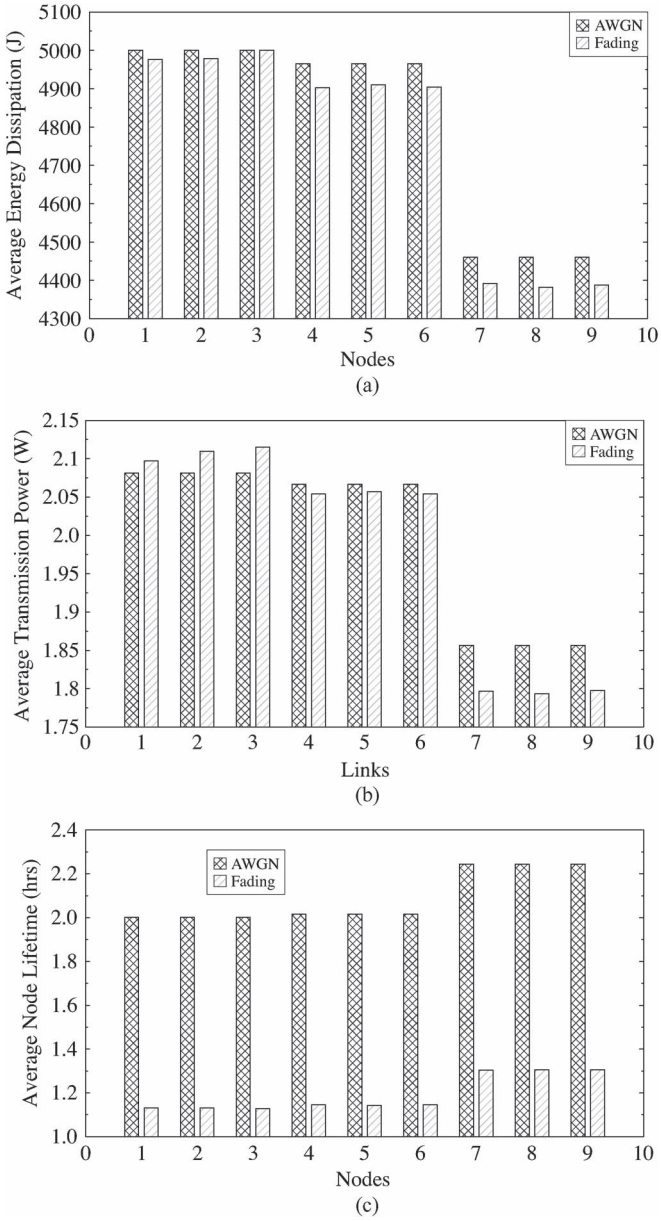

Fig. 5. Energy dissipation per node, average transmit power per link and lifetime of all nodes in the network in both AWGN and fading channels for the $T = 3$ link schedule at a source rate of 0.29 bits/s/Hz. (a) Energy dissipation per node. (b) Average transmit power per link. (c) Lifetime of all nodes in the network.

Furthermore, we comprehensively study the energy dissipation per node, the average transmission power per link, and the lifetime of all sensor nodes in the network. Fig. 5 shows the energy dissipation per node, the average transmission power per link, and the lifetime of all nodes in the network in both AWGN and fading channels for the $T = 3$ link schedule of Fig. 2 at a source rate of 0.29 bits/s/Hz. In the network

topology considered, the transmissions from the first three nodes suffer from the highest amount of interference. This is because their receiving nodes are closer to their potential interferers, when compared with any other sets of nodes. Therefore, to satisfy the flow conservation constraints, these nodes must transmit at higher power, as shown in Fig. 5(b). Thus, in an AWGN channel, the first three nodes in the network dissipate their 5000-J initial amount of energy faster than the other nodes since the energy dissipation is proportional to the transmit power, as shown in Fig. 5(a), whereas in the Rayleigh block-fading channel, the third node runs out of battery first, which also determines the lifetime of the WSNs. The required transmit power of the third link is higher than that in the AWGN channel scenario. This increase in transmit power is required to overcome the effect of fading.

The average transmit power per link is calculated by summing the transmit power values per link and then by dividing it by the number of TSs that the same link was allowed to transmit. For the first three links operating in the AWGN channel, the required transmission power per link is higher than that of the rest of the links. Since requiring a high transmit power results in dissipating more energy, the lifetime of those nodes is reduced, as shown in Fig. 5(c).

Upon comparing the AWGN and fading channel scenarios in Fig. 5, we observe that they follow a similar trend. An observation is that the average transmit power per link of the seventh, eighth, and ninth nodes in Fig. 5(b) is slightly lower for the fading channel than for the AWGN channel. However, interestingly, the average transmit power per link of the third node in Fig. 5(b) recorded for the fading channel is slightly higher than that of the AWGN channel. Therefore, the need for a high transmit power necessitates higher energy dissipation for that particular node. Hence, the NL is reduced, which can also be observed by comparing Figs. 3 and 4. Fig. 3 shows that the NL of the WSN in the AWGN channel recorded for the $T = 3$ link schedule and for 0.29 bits/s/Hz source rate is approximately 2 h. By contrast, Fig. 4 shows that the NL of the WSN operating in a Rayleigh fading scenario for the $T = 3$ link schedule and for 0.29-bits/s/Hz source rate indicates approximately an NL of 1.13 h. This earlier node failure of the fading scenario is due to the poor channel conditions, where the fading required higher transmit power in the third node, as shown in Fig. 5(b). Therefore, this earlier node failure shortened the NL of the WSNs in fading channels.

To put the given results into context, we apply our analysis to the environmental sensor networks of [28], where the relation between glaciers and climate change was studied. In their work, Martinez *et al.* [28] transmit data only once per day for a 0.5-s time slot. In this specific application and considering our results in Fig. 5 for $T = 3$ and a source rate of 0.29 bits/s/Hz, the battery will serve communications for 7200 s, which means that the NL will be around four years and three months in the LOS AWGN channel. We also consider what NL we can achieve if the environmental conditions are more challenging and the channel is exposed to the severe environments mentioned in [28], which may be modeled by a non-LOS Rayleigh block-fading channel. Activating the communication channel once per day in fading conditions will lead us to an NL of around two years and six months.

V. Conclusion

We evaluated the optimal NL in an interference-limited scenario for an optimal transmit rate and power, when considering the so-called spatially periodic time sharing scheme of Fig. 2. The maximization of NL was formulated as a nonlinear optimization problem taking into account the link scheduling, the transmission rates, and transmit power of all active TSs. The original nonlinear problem was converted into a convex optimization problem by employing an approximation of the SINR. We then derived the Lagrangian form of the convex optimization problem and employed the KKT optimality conditions [24] for deriving analytical expressions of the globally optimal transmit rate and power for our specific network topology. Finally, we obtained the maximum NL for both AWGN and Rayleigh fading channels. Our numerical results illustrated that fading has a detrimental impact on the achievable NL due to the poor channel conditions that require an increased transmit power to combat the effects of the fading. Furthermore, the simultaneous scheduling of links that interfere only weakly allowed us to take advantage of spatial reuse, where the activation of simultaneous transmissions at reduced rates necessitates reduced transmission power, which results in extending the NL. From this paper, we can conclude that the choice of scheduling depends on the application since a lower source rate favors infrequent transmissions requiring low transmit power, which do not suffer from interference, when aiming for extending the NL. However, for higher source rates, a higher NL can be achieved by aggressive spatial reuse.

Given the limitations of the centralized solution approach mentioned in Section III-B, the focus of this paper is on the information delay analysis. We also plan to extend our string topology model to a random network topology, where a single string (SN–DN pair) can be assumed to constitute a single route of the random topology. Nonetheless, conceiving distributed solutions for avoiding the limitations of our centralized scheme constitutes attractive future research directions.

References

[1] I. Dietrich and F. Dressler, "On the lifetime of wireless sensor networks," *ACM Trans. Sensor Netw.*, vol. 5, no. 1, pp. 5:1–5:39, Feb. 2009.

[2] W. Liu, K. Lu, J. Wang, G. Xing, and L. Huang, "Performance analysis of wireless sensor networks with mobile sinks," *IEEE Trans. Veh. Technol.*, vol. 61, no. 6, pp. 2777–2788, Jul. 2012.

[3] J. Chen, J. Li, and T. Lai, "Trapping mobile targets in wireless sensor networks: An energy-efficient perspective," *IEEE Trans. Veh. Technol.*, vol. 62, no. 7, pp. 3287–3300, Sep. 2013.

[4] M. Najimi, A. Ebrahimzadeh, S. Andargoli, and A. Fallahi, "Lifetime maximization in cognitive sensor networks based on the node selection," *IEEE Sensors J.*, vol. 14, no. 7, pp. 2376–2383, Jul. 2014.

[5] J. Du, K. Wang, H. Liu, and D. Guo, "Maximizing the lifetime of k-discrete barrier coverage using mobile sensors," *IEEE Sensors J.*, vol. 13, no. 12, pp. 4690–4701, Dec. 2013.

[6] H. Salarian, K. Chin, and F. Naghdy, "An energy-efficient mobile-sink path selection strategy for wireless sensor networks," *IEEE Trans. Veh. Technol.*, vol. 63, no. 5, pp. 2407–2419, Jun. 2014.

[7] J. W. Jung and M. Weitnauer, "On using cooperative routing for lifetime optimization of multi-hop wireless sensor networks: Analysis and guidelines," *IEEE Trans. Commun.*, vol. 61, no. 8, pp. 3413–3423, Aug. 2013.

[8] Y. Chen and Q. Zhao, "On the lifetime of wireless sensor networks," *IEEE Commun. Lett.*, vol. 9, no. 11, pp. 976–978, Nov. 2005.

[9] C. Cassandras, T. Wang, and S. Pourazarm, "Optimal routing and energy allocation for lifetime maximization of wireless sensor networks with nonideal batteries," *IEEE Trans. Control Netw. Syst.*, vol. 1, no. 1, pp. 86–98, Mar. 2014.

[10] D. Yuan, V. Angelakis, L. Chen, E. Karipidis, and E. Larsson, "On optimal link activation with interference cancelation in wireless networking," *IEEE Trans. Veh. Technol.*, vol. 62, no. 2, pp. 939–945, Feb. 2013.

[11] Z. Yang, Q. Zhang, and Z. Niu, "Throughput improvement by joint relay selection and link scheduling in relay-assisted cellular networks," *IEEE Trans. Veh. Technol.*, vol. 61, no. 6, pp. 2824–2835, Jul. 2012.

[12] R. Madan, S. Cui, S. Lall, and A. Goldsmith, "Cross-layer design for lifetime maximization in interference-limited wireless sensor networks," *IEEE Trans. Wireless Commun.*, vol. 5, no. 11, pp. 3142–3152, Nov. 2006.

[13] A. Goldsmith, *Wireless Communications*. Cambridge, U.K.: Cambridge Univ. Press, 2005.

[14] H. Yetgin, K. T. K. Cheung, and L. Hanzo, "Multi-objective routing optimization using evolutionary algorithms," in *Proc. IEEE WCNC*, Paris, France, Apr. 2012, pp. 3030–3034.

[15] L. Van Hoesel, T. Nieberg, J. Wu, and P. J. M. Havinga, "Prolonging the lifetime of wireless sensor networks by cross-layer interaction," *IEEE Wireless Commun. Mag.*, vol. 11, no. 6, pp. 78–86, Dec. 2004.

[16] H. Kwon, T. H. Kim, S. Choi, and B. G. Lee, "A cross-layer strategy for energy-efficient reliable delivery in wireless sensor networks," *IEEE Trans. Wireless Commun.*, vol. 5, no. 12, pp. 3689–3699, Dec. 2006.

[17] H. Nama, M. Chiang, and N. Mandayam, "Utility-lifetime trade-off in self-regulating wireless sensor networks: A cross-layer design approach," in *Proc. IEEE ICC*, Istanbul, Turkey, Jun. 2006, vol. 8, pp. 3511–3516.

[18] J. Zhu, S. Chen, B. Bensaou, and K.-L. Hung, "Tradeoff between lifetime and rate allocation in wireless sensor networks: A cross layer approach," in *Proc. 26th IEEE INFOCOM*, Anchorage, AK, USA, May 2007, pp. 267–275.

[19] S. Ehsan, B. Hamdaoui, and M. Guizani, "Radio and medium access contention aware routing for lifetime maximization in multichannel sensor networks," *IEEE Trans. Wireless Commun.*, vol. 11, no. 9, pp. 3058–3067, Sep. 2012.

[20] P. Li, S. Guo, and V. Leung, "Maximum-lifetime coding tree for multicast in lossy wireless networks," *IEEE Wireless Commun. Lett.*, vol. 2, no. 3, pp. 295–298, Jun. 2013.

[21] J.-H. Jeon, H.-J. Byun, and J.-T. Lim, "Joint contention and sleep control for lifetime maximization in wireless sensor networks," *IEEE Commun. Lett.*, vol. 17, no. 2, pp. 269–272, Feb. 2013.

[22] X. Liu, "A transmission scheme for wireless sensor networks using ant colony optimization with unconventional characteristics," *IEEE Commun. Lett.*, vol. 18, no. 7, pp. 1214–1217, Jul. 2014.

[23] H. Wang, N. Agoulmine, M. Ma, and Y. Jin, "Network lifetime optimization in wireless sensor networks," *IEEE J. Sel. Areas Commun.*, vol. 28, no. 7, pp. 1127–1137, Sep. 2010.

[24] S. P. Boyd and L. Vandenberghe, *Convex Optimization*. Cambridge, U.K.: Cambridge Univ. Press, 2004.

[25] A. Goldsmith and S.-G. Chua, "Variable-rate variable-power MQAM for fading channels," *IEEE Trans. Commun.*, vol. 45, no. 10, pp. 1218–1230, Oct. 1997.

[26] M. Albulet, *RF Power Amplifiers*. Raleigh, NC, USA: SciTech, 2001.

[27] D. Palomar and M. Chiang, "A tutorial on decomposition methods for network utility maximization," *IEEE J. Sel. Areas Commun.*, vol. 24, no. 8, pp. 1439–1451, Aug. 2006.

[28] K. Martinez, J. Hart, and R. Ong, "Environmental sensor networks," *Computer*, vol. 37, no. 8, pp. 50–56, Aug. 2004.

AUTHOR QUERIES

AUTHOR PLEASE ANSWER ALL QUERIES

AQ1 = Please provide keywords.

END OF ALL QUERIES